Syngas Production from Electrochemical Reduction of CO2: Current Status and Prospective Implementation

Green Chemistry

Accepted Manuscript

This article can be cited before page numbers have been issued, to do this please use: S. Hernandez, M. A. Farkhondehfal, F. Sastre, M. Makkee, G. Saracco and N. Russo, *Green Chem.*, 2017, DOI: 10.1039/C7GC00398F.

ROYAL SOCIETY OF CHEMISTRY

rsc.li/green-chem

DOI: 10.1039/C7GC00398F

Syngas Production from Electrochemical Reduction of CO_2: Current Status and Prospective Implementation

Simelys Hernández,[a,b,*] M. Amin Farkhondehfal,[a] Francesc Sastre,[c] Michiel Makkee,[c] Guido Saracco,[b] and Nunzio Russo[a]

[a] Applied Science and Technology Department, Politecnico di Torino, C.so Duca degli Abruzzi 24, Turin 10129, Italy

[b] Center for Sustainable Future Technologies, CSFT@POLITO, Italian Institute of Technology, C.so Trento 21, Turin 10129, Italy.

[c] Catalysis Engineering, Dept. of Chemical Engineering, Faculty of Applied Sciences, Delft University of Technology, Van der Maasweg 9 , 2629 HZ Delft, The Netherlands.

[*] Corresponding author: simelys.hernandez@polito.it; Tel.: +39-011-0904774

Abstract

The CO_2 that comes from the use of fossil fuels accounts for about 65% of the global greenhouse gases emissions, and it plays a critical role in global climate changes. Among the different strategies that have been considered to address the storage and reutilization of CO_2, the transformation of CO_2 into chemicals or fuels with a high added-value has been considered a winning approach. This transformation is able to reduce the carbon emissions and induce a "fuel switching" that exploits renewable energy sources. The aim of this brief review is to gather and critically analyse the main efforts that have been made and achievements that have been reached in the electrochemical reduction of CO_2 for the production of CO. The main focus is on the prospective of exploiting the intrinsic nature of the electrolysis process, in which CO_2 reduction and H_2 evolution reactions can be combined, into a competitive approach, to produce syngas. Several well-stablished processes already exist for the generation of fuels and fine-chemicals from H_2/CO mixtures of different ratios. Hence, the different kinds of electrocatalysts and electrochemical reactors that have been used for the CO and H_2 evolution reactions have been analysed, as well as the main factors that influence the performance of the system from the thermodynamic, kinetic and mass transport points of view.

Keywords: Syngas productions, renewable energy, electrochemical reduction of CO_2, H_2/CO ratio.

View Article Online
DOI: 10.1039/C7GC00398F

1. Introduction

About 65% of the global greenhouse gases (GHG) emissions are constituted by CO_2 that comes from both the use of fossil fuels and industrial processes, such as cement manufacturing (see Fig. 1). In fact, the current energy system in the Earth relies above all on non-sustainable fuels (*i.e.* oils, coal, and natural gas) for the production of electricity and heat in different fields, e.g. industry, transportation, buildings heating and others, which cause the generation of 94% of the global GHG emissions. Moreover, it is now widely accepted that the rising levels of carbon dioxide (CO_2) are considered one of the main reasons for global warming.[1, 2] Therefore, over the last two decades, international governmental regulations and R&D programs have attempted to limit GHG emissions. The main aim of the Paris agreement, signed in December 2015 by the representatives of 195 countries during the 21st Conference of Parties on Climate Change (COP21), is to significantly reduce the risks and impacts of climate changes. The main objective is to keep the rise in global temperature well below 2 °C during this century, with respect to pre-industrial levels, and to pursue efforts to limit the temperature increase even more to 1.5 °C.[3]

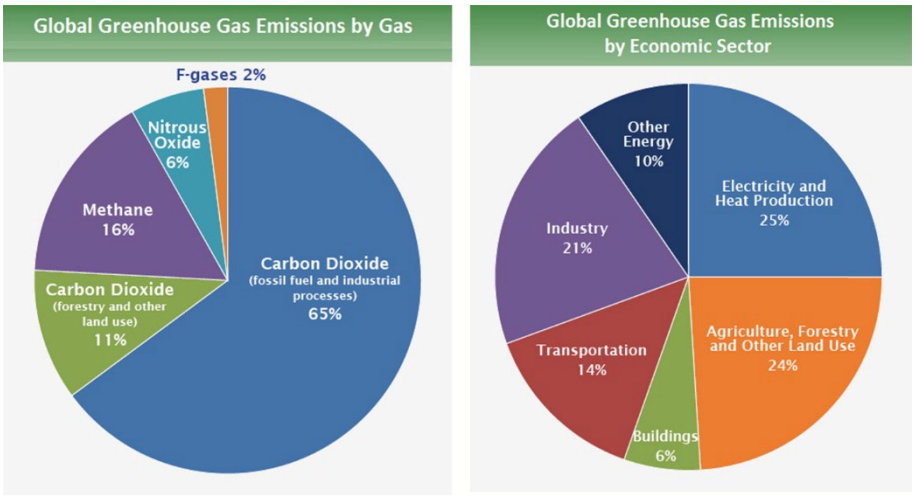

Figure 1. Global GHG emissions produced by human activities and categorized on the basis of the economic sectors that lead to their production. Source: IPCC (2014) based on emissions in 2010. [2]

In addition to climate change issues, it is know that fossil fuel resources are not evenly distributed and are depleting,[4] and this has led to geographical constrains and an insecurity about the supply of energy throughout the world. Therefore, the deployment of an alternative carbon cycle, which includes the production of alternative fuels (the so called "fuel switching"), is currently a great challenge. In such a way, the three main three overarching energy and climate policy objectives, that is, security of supply, competitiveness, and sustainability, which were defined in the European Energy Security Strategy Plan, have a chance of being reached.

Different strategies have been put in place by the scientific community in order to address the CO_2 storage[5] and reuse.[6] Among them, producing more energy from renewable sources and using fuels with lower carbon contents than fossil fuels are two winning ways of reducing fossil carbon emissions. In the latter case, the challenge concerning the reduction of the carbon footprint can be faced through both the reuse of CO_2 and the exploitation of intermittent renewable energy sources (*i.e.* sunlight, wind, *etc*.) and storing their power in chemicals or fuels. Moreover, the effectively implementation of alternative liquid fuels would be easier than for other renewable fuels, such as the H_2, since it would not require an overall change of the existing energetic system at the storage, transport, and

View Article Online
DOI: 10.1039/C7GC00398F

distribution levels. Nevertheless, the industrial transformation of CO_2 to fuels is currently at a low level due to the lack of efficient and cost-effective processes that also offer good scalability.[7]

Among all the proposed methods, the electrochemical reduction of CO_2 can be considered an interesting technology for the storage and reutilization of CO_2 from both an economic and an environmental points of view.[7] It can be used to transform CO_2 into CO, formic acid, alcohols or higher molecular weight hydrocarbons, such as oxalic acid. However, the main challenge for the establishment of this technology, at an industrial level, is to find suitable electro-catalysts as well as optimized process conditions for the selective production of a single compound with a high conversion efficiency.

Owing to the increasing attention that CO_2 reduction has gained over the last few years, many reviews have been published with the aim of to summarizing the efforts that have been made.[8-11] For instance, Jones *et al.*[7] examined the mechanisms of CO_2 reduction on metal surfaces in detail, and summarized the most representative results on the production of formate, CO and higher molecular weight hydrocarbons, in both water and non-aqueous electrolytes under pressure, and using molecular catalysts. Fenwick *et al.* [8] analysed the electrochemical reduction of N_2 and CO_2 on molecular (homogeneous) and heterogeneous catalysts, focusing on the current technical challenges for the creation of an integrated solar fuel device. Hu *et al.*[12] summarised the different methods for the thermal, electrochemical, and photochemical conversion of CO_2 to fuels and other value-added products (*i.e.* oxygen-rich compounds and polymers). Photocatalytic and photo-electrochemical CO_2 reduction have also recently been addressed by Li *et al.*[13] and Akhter *et al.*[14] Nonetheless, no specific focus on the production of syngas (a mixture of H_2 and CO) has been reported in the open literature or the public domain. A straightforward and cost-effective electrochemical process for the production of syngas from renewable power would open the way towards a well-established form of chemistry for the synthesis of a variety of hydrocarbon fuels in order to substitute fossil fuels without the need to change of the current distribution infrastructures.

Therefore, the aim of this review has been to gather and critically analyse the main efforts that have been made and results that have been achieved concerning the electrochemical reduction of CO_2 for the production of CO. The advantages of this technological approach, with respect to the generation of other products, have been analysed from the kinetic and thermodynamic points of views. Moreover, the different methods, catalysts and reactor systems that have been used for this purpose, as well as the challenges and prospective trends towards a practical application of this technology have been outlined.

2. Syngas from CO_2: The Opportunity

Since the electrochemical reduction of CO_2 is generally performed in aqueous media, the hydrogen evolution reaction (HER) from the reduction of water or protons (H^+) is in inevitable rivalry with the CO_2 conversion. Hence, the intrinsic nature of the electrolysis process could be exploited, in a competitive approach, by combining CO_2 reduction and HER for the production of syngas. This would allow well-known and robust options to be used for the downstream processing of syngas in order to generate ammonia or more reduced products, such as alcohols and hydrocarbons (*e.g.* via heterogeneous Fischer-Tropsch catalysis).[7, 15]

The great advantage of producing syngas, instead of another direct CO_2 reduction product, is the fact that the are several possible options for further developments of engineered products in relations to the H_2/CO ratio of the mixture. In such an approach, both the electrochemical reactor configuration

and the catalyst compositions play a key roles in the production rates of both H_2 and CO, as will be discussed in detail in the next sections. Subsequently, depending on its composition, the syngas can be used to generate different derivatives or fuels. As shown in Fig. 2, it can be used as feedstock or as an intermediate for the production of bulk chemicals, fertilizers, pharmaceutical, plastics, solvents and chemical intermediates (*e.g.* NH_3, methanol). For example, ammonia is employed in the production of fertilizers, and methanol is exploited in the manufacturing of liquid fuels and chemicals, such as formaldehyde, acetic acid, and dimethyl ether (DME). It has emerged, from the recent "Syngas & Derivatives: A Global Strategic Business Report" by Global Industry Analysts Inc.,[16] that developing countries are the leading markets throughout the world, and Asia-Pacific, Middle East and African countries account for more than two-thirds of the global consumption of syngas. Moreover, the rising demand for methanol in China, owing to the recent establishment of methanol-to-olefin and methanol-to-propylene plants, has resulted in further significant opportunities for the production of syngas from renewable energy sources. In fact, the Asia-Pacific market of syngas had the fastest annual growth rate of 3.2% in the 2007-2013 period.[16] Moreover, syngas is used widely as a fuel in internal combustion engines to generate for electricity and as an intermediate in the production of synthetic natural gas (CH_4), biodiesel, and other fuels. Thus, the global consumptions of syngas and its derivatives has been forecasted to reach 146 thermal GW by 2020,[16] because of the increasing demand for major end-use applications, including transportation fuels, chemical intermediates and fertilizers.

The known increasing global demands for fuel and electricity, driven by the world's expanding population, the increasing use of electrical and electronical devices, as well as the rising concerns about global warming and greenhouse gases emissions are driving attention towards alternative fuels. These issues, in addition to the current growth in the exploitation of syngas, which is driven by the increasing on the use of syngas derivatives, offer opportunities that could be exploited throughout the world. Therefore, it is believed that the continuous growth in the renewable energy sector will be exploited to make use of syngas for the production of fuels and chemicals.

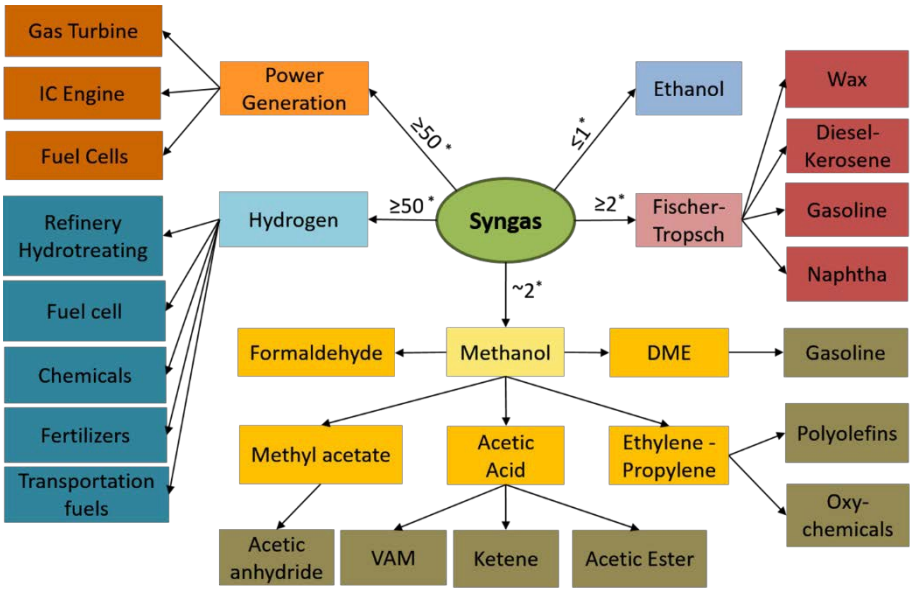

Figure 2. Syngas derivatives with reference to its composition (* H_2/CO molar ratio)

View Article Online
DOI: 10.1039/C7GC00398F

3. State-of-the-art of Electrochemical Reduction of CO_2 to CO in Heterogeneous Catalysts

3.1. The thermodynamics of CO_2 reduction

As the CO_2 molecule is rather stable, a significant amount of energy is required to convert it into valuable products (free Gibbs formation energy: ΔG = -394 kJ/mol in gas phase).[14] Table 1 summarises the free energy changes and the standard Nernst potentials (E^o) vs. Normal Hydrogen Electrode (NHE) (at 25 °C, 1 bar, pH=7) necessary for the conversion of CO_2 to different products. Since these reactions take place by means of reduction protonation and not hydrogenation,[17] the variation in the redox potential with temperature can be calculated through the Gibbs- Helmholtz relationship:

$$E(T) = \frac{-\Delta G}{nF} = -\frac{(\Delta H(T) - T\Delta S(T))}{nF} \qquad (1)$$

where G is the Gibbs free energy, H is the enthalpy, and S is the entropy.

The entropy contribution, through the term (–TΔS) in the Gibbs- Helmholtz relationship, is negligible as far as the thermodynamic driving force necessary for the reaction at room temperature is concerned, and the value of the enthalpy change ΔH is therefore a good indicator of thermodynamic feasibility.[18] It is clear, from Table 1, that none of the CO_2 reductions reactions requires a large potential, except for the formation of the $CO_2^{\bullet -}$ radical, which is defined as an intermediate for the generation of some products, such as CO, formic acid, and methane. However, despite the thermodynamic feasibility of reducing CO_2, certain kinetic barriers hinder the multi-electron reduction processes, cause high overpotentials and limit the reaction. As a result, the reduction of CO_2 in aqueous solutions is expected to be accompanied, or even replaced, by the kinetically more favourable H_2 evolution reaction.[14]

Table 1. The standard ΔG° (25°C; pH = 0) and standard Nernst potentials (E^o) at 25 °C, 1 bar and pH=7 [19]

Reaction	ΔG^0 (kJ/mol)	E^0 (V vs. NHE)
$CO_2 + 2H^+ + 2e^- \rightarrow CO + H_2O$	19.9	-0.53
$CO_2 + 2H^+ + 2e^- \rightarrow HCOOH$	38.4	-0.61
$CO_2 + 4H^+ + 4e^- \rightarrow H_2CO + H_2O$	27.5	-0.48
$CO_2 + 8H^+ + 8e^- \rightarrow CH_4 + 2H_2O$	-130.8	-0.38
$CO_2 + 6H^+ + 6e^- \rightarrow CH_3OH + H_2O$	-17.3	-0.24
$CO_2 + e^- \rightarrow CO_2^{\circ -}$	183.32	-1.9

Theoretically, CO_2 can be reduced in an aqueous solution to form carbon monoxide, formic acid, methane or other hydrocarbons by means of a minimum thermodynamic cell potential between 1.47 V and 1.94 V (considering water oxidation as the anodic reaction, E^o = 1.23V *vs.* NHE). However, a higher cell potential needs to be applied to initiate the CO_2 reduction in order to overcome the overpotentials of the system.[20] The overpotential of an electrochemical reaction is defined as the potential difference between the thermodynamic reduction potential of the half-reactions and the potential at which the redox event is experimentally observed.[21] In CO_2 reduction reactions, the overpotentials are mainly caused by: (a) the activation energy needed for the electron transfer to the CO_2 molecule, (b) ohmic losses due to electrolyte and electrode conductivity, and (c) mass transport limitations.[22] Of all the CO_2 reduction

products, CO is the most likely and easiest to occur from the thermodynamic point of view, because only two electrons are involved in the reaction (see Table 1). However, as can be noted in Fig. 3, the overpotentials reported in literature for the CO_2 reduction to CO range from between few mV and about 3 V, depending on which electrocatalysts are employed. The details and performances achieved with different kinds of electrocatalysts materials that have been specifically developed for a selective production of CO are summarized in section 4.1.

The most common parameters employed to report the performances of CO_2 reducing electrocatalysts are summarized in the section 3.2. Moreover, since one of the main reasons for the high overpotentials regards the CO_2 reduction mechanism, more details on this aspect are given in section 3.3.

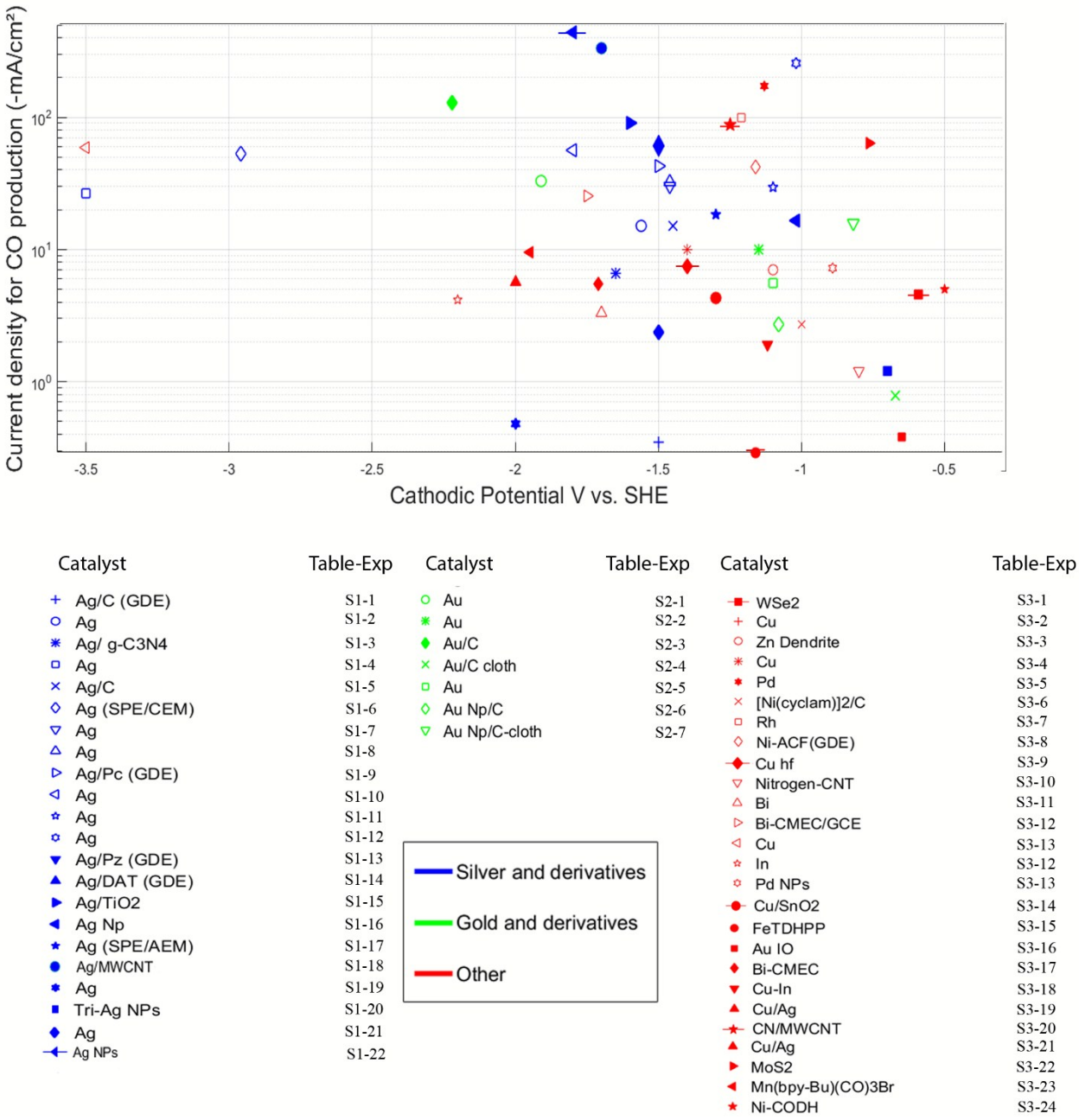

Figure 3. Maximum cathodic current densities achieved for the CO_2 electrochemical reduction to CO (as the main C-based product) with different catalytic systems *versus* the applied cathodic potential. The catalysts in the legend are colour classified according to the type of metal (*i.e.* Ag in blue, Au in green and others in red).

View Article Online
DOI: 10.1039/C7GC00398F

More details about each specific catalysts and its testing conditions are summarized in the next sections and Tables, as reported in the legend. Exp: experiment indicated in each table.

3.2. Quantification of the Efficiency of the Electrodes

The current density is the parameter that is used the most to define the performance of an electrocatalyst. It is defined as the electric current per unit of surface or geometric area of the electrode, and it is a vector whose magnitude is the electric current per cross-sectional area at a given point in space and applied potential.[23] The higher is the current density at a given potential is, the higher the reaction rate of the electrochemical reaction. A collection of the best current densities achieved for the different CO_2 reduction catalysts and systems aimed at generating CO as the main product are given in Fig. 3, together with the applied cathode potential. As is known, the lower the potential is (in absolute value term), the lower the overpotential for the reaction in such a system. Hence, the most desired electro-catalyst/reactor configuration should produce a high current density (related to CO production) at a potential as close as possible to the E^o, *i.e.* -0.53V *vs* SHE (the condition of zero overpotential).

The exchange current density is a current without net electrolysis and with a zero overpotential. The exchange current can be considered a background current to which the net current observed at various overpotentials is normalized. The electron transfer processes of a redox reaction, written as a reduction in the equilibrium potential, continues at the electrode/solution interface in both directions, and the current density is therefore the electric current per unit area of the cross section.[24]

In addition, it is quite normal to obtain different CO_2 reduction products (e.g. CO, CH_4, etc.) and side-products (*e.g.* H_2). Thus, in order to obtain knowledge about the selectivity of a catalyst, it is essential to quantify the relative formation of CO with respect to all the products. The yield of an electrochemically generated product is expressed in terms of the so-called Faradaic efficiency (FE), which is the most commonly used parameter to describe the electrochemical selectivity and the occurrence of product cross-over.[25] FE is defined as the ratio of the number of coulombs required to form a certain amount of product (determined by chemical analysis) to the total charge over a specific time interval. The Faradic efficiency for CO production can be calculated as:

$$FE = \frac{2 \cdot F \cdot mol\ CO\ produced}{j \cdot A \cdot t} \qquad (2)$$

where *F* is the Faraday constant (96485.33 s A/mol), *j* is the current density (A/m^2), A is the electrode area (m^2), and *t* is the reaction time (s).

Ideally, the sum of the FEs of all the products should be 100 %, in order to obtaine a Faradic balance. The attainment of the Faradic balance is the first step in any kinetic study of any electrochemical reaction system. Nevertheless, many of the research works (even some of those described in Fig. 3) have reported the FE for CO production without giving a detailed analysis of the side products.

Another figure of merit that defines the practical applicability of a specific electrocatalysts is the production rate (PR), which defines the reaction rate necessary to obtain a particular product. The CO production rate, at a given applied potential, can be calculated as:

$$PR = \frac{j \cdot FE}{2 \cdot F} \qquad (3)$$

Although the PR is not usually reported, because the selectivity of CO_2 reduction electrocatalysts sometimes changes over time,[26] it is an important parameter that should be calculated, under steady-state conditions, after long lasting experiments, for practical implementation of the reaction at a large scale.

3.3. CO_2 reduction mechanism on metal electrodes

The kinetic barriers to CO_2 activation can be overwhelmed by finding catalysts that are able to break down the linear symmetry of the CO_2 molecule and favour the formation of the C–H bond, that is, the so called proton-coupled electron transfer.[22] Thus, materials that are able to catalyse the more favourable multi-electron and multi-proton reactions are needed to improve the CO_2 reaction kinetics.[25]

As shown in the Fig. 4, different metal electrodes have been adopted to obtain the selective reduction of CO_2 to a specific product. A change in the geometry of CO_2, that is, from a linear to a bent CO_2 or $CO_2^{\bullet -}$, is necessary to obtain its initial reduction and leads to a significant overpotential in the CO_2 reduction.[19] The formation of the $CO_2^{\bullet -}$ intermediate is considered very important, as it is the first and rate limiting step, and its coordination determines whether the 2e- reduction will proceed towards the production of either CO or formate.[27] The high energy demand of the $CO_2^{\bullet -}$ (-2.21 V *vs* SCE) to interact with water (to produce CO or formate), another CO_2 molecule or its derivatives and subsequent reactions, is considered instantaneous compared to the first step.[7, 28] Therefore, the stabilization of this intermediate plays a key role in both the efficiency and reaction rate of the CO_2 reduction process.

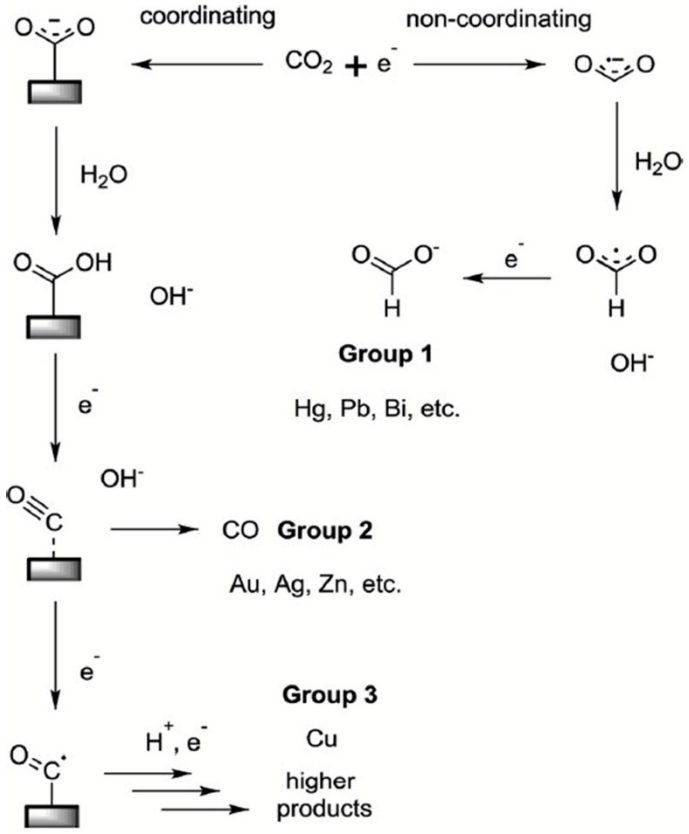

Figure 4. Electrochemical CO_2 reduction mechanism on metal surfaces with water. Reproduced with permission from Ref. [7] with the kind permission of John Wiley and Sons. Copyrights 2014.

View Article Online
DOI: 10.1039/C7GC00398F

In a recent work, J.P. Jones *et al.*[7] have categorized the type of electrodes in three groups, according to their tendency to bind the $CO_2^{\bullet-}$ intermediate and to whether they are able to reduce CO (see Fig. 4). Group 1 is constituted by metals such as Pb, Hg, In, Sn, and Cd, which neither bind the $CO_2^{\bullet-}$ intermediate nor reduce the CO, thus producing formate (or formic acid) as the main product. Group 2 consists of catalysts such as Au, Ag, Zn, and Ga, which are able to bind the $CO_2^{\bullet-}$ intermediate, but cannot reduce CO, and thereby produce various degrees of CO yield.[29] Copper is the only metal that belongs to in group 3, because it is able to both bind $CO_2^{\bullet-}$ and reduce CO to higher molecular weight products, such as alcohols and hydrocarbons.[30, 31] Other metals, such as Ni, Fe, Pt, and Ti are more likely to be excluded from the reduction of CO_2 in aqueous media because they are highly active in reducing water (H^+), and thus favour the H_2 production.[7, 32]

Another alternative that has gained a great deal of attention in recent works is the use of ionic liquids (usually N-containing salts), which are adopted to manipulate the above mechanisms and to improve the CO_2 reduction rate. As mentioned above, the equilibrium potential for $CO_2^{\bullet-}$ formation as an intermediate radical is high. The role of ionic liquids is to reduce the potential of $CO_2^{\bullet-}$ formation, most likely by complexation via a weak bonding between CO_2 and the anions of the ionic liquid`s (e.g. BF_4^-, $PF6^-$).[12, 33] Fig. 5 shows how the CO_2 can interact with a commonly used ionic liquid anion (*i.e.* BF_4^-) to generate a slightly bent intermediate complex that then undergoes electrolysis. CO is the main reaction product in most non-aqueous systems, regardless of the electrode material. The absence of water obviously limits the production of formate, and the products differ drastically from the aqueous case. However, in some cases, water can still be present in the system, and can be mixed with the ionic liquids as a way of reducing costs and diminishing the viscosity of the solution.

(4)

Figure 5. Schematic interaction between CO_2 and BF_4^-. Reproduced from Ref. [7] with the kind permission of permission of John Wiley and Sons. Copyrights 2014.

4. Syngas production

As mentioned above, syngas consists of a mixture of CO and H_2, both of which are the main products of the CO_2-water electrochemical reduction, because of the standard reduction potentials of such reactions (*i.e.* -0.41 V and -0.54 V *vs* NHE at pH 7.0 for H_2 and CO production, respectively). Hence, when reducing CO_2 in aqueous media, the concomitant generation of H_2 is almost unavoidable. Therefore, the selection of both the catalyst and the operation conditions plays an important role in the tuning of the H_2/CO ratio that is produced during the reaction. Nevertheless, most of the efforts over the last few years have been focused on the development of an appropriate catalysts for the selective CO production. The main challenge has been to find a suitable CO_2 reduction catalyst with: (i) a high selectivity towards CO (*i.e*. high Faradaic efficiency) rather than other side products, (ii) an adequate rate of reaction (*i.e*. current density) for scaling up, (iii) good stability for a constant productivity over time. Different metals have been studied as catalysts for this purpose, as discussed in the next sub-sections.

4.1. CO production from electrochemical CO_2 reduction

Au and Ag are the most favourite metals for the electrochemical selective reduction of CO_2 to CO, due to their inability to reduce CO to other side products. One of the problems of these catalysts is the

View Article Online
DOI: 10.1039/C7GC00398F

high cost of such noble-metals. Therefore, the use of nanoparticles supported on different materials is a logical way of reducing the cost of such electrodes, as well as of improving both their stability and their conversion efficiency. The use of co-catalysts and different support materials has also been applied as a way of stabilizing small nanoparticles, of increasing catalysts dispersion and utilization, and of enhancing electron conductivity and mass transport.[34, 35] Moreover, some specific materials have been used as electro-catalysts supports, and have led to certain advantages, such as reducing the electrode overpotential.[36] Other kinds of materials have also been employed with the aim to substituting Ag and Au materials. In most of these studies, the main focus has been on maximizing the current densities, and as a result, the operative conditions have also been changed. Hence, different studies are summarized and critically addressed in the next sections on the basis of the type of catalyst and the process conditions.

4.1.1. Ag based electrodes

Ag can be considered a promising material because it is less expensive than other noble metal catalysts. The price of pure silver (~ 15.5 €/oz), for example, is about 72 and 58 times lower than that of pure gold (~1112 €/oz) and platinum (~ 906 €/oz), respectively.[37] The metallic surface of Ag has shown a good activity and selectivity towards converting CO_2 into CO in aqueous electrolytes.[36, 38-40] This reduction takes place with a smaller overpotential than that of many other metallic surfaces.[41] Table S1 (in the supporting information, *SI*) summarizes the main experimental conditions and the best results reported for CO generation accomplished with Ag based electro-catalysts. It should be pointed out that the current density values shown in Table S1 (*SI*) are related to the overall electrochemical process and does not take into account the specific selectivity toward H_2, CO or any other sub-products. Therefore, for better comparison purposes, Fig. 6 shows the current densities and the Faradaic efficiencies for the CO production of such materials.

The problems concerning the use of Ag as a catalyst are its low abundance and high cost, compared to other earth-abundant elements (*i.e.* Mn, Ni, Co, Fe), as well as the high overpotentials induced by the use of this material in its bulk form (*i.e.* Ag foils, see Table S1, *SI*). The dispersion of Ag in the form of nanoparticles (NPs) on different substrates and the use of co-catalysts have been introduced to overcome these challenges, to better utilize the Ag surface and to construct high-performing electro-catalysts. Lu *et al*.[41] developed a de-alloying process to synthesize a nano-porous Ag catalyst with a monolithic structure and highly curved inner surfaces. They achieved a current density of 18 $mA{\cdot}cm^{-2}$ at 500 mV of overpotential and 92 % of Faradaic efficiency under atmospheric pressure conditions. Liu *et. al*[42] have demonstrated a predominant shape-dependent electrocatalytic reduction of CO_2 to CO on triangular silver (Tri-Ag) nanoplates, with a high Faradic efficiency (96.7 %) and energy efficiency (61.7 %), but with a low current density and production rate.

Among the different substrates, TiO_2 is frequently used because it can also be used as a co-catalysts in the photo-electro-chemical reduction of CO_2.[25, 43, 44] Kenis *et al.*[36] synthesized Ag nanoparticles supported on TiO_2 and tested them to establish their CO_2 electro-chemical reduction capacity. They found that 40 wt % Ag/TiO_2 NPs can reach a CO Faraday efficiency of 90 %, with a current density of -101 $mA{\cdot}cm^{-2}$. They have also recently reported a significant improvement of current density (up to 350 $mA{\cdot}cm^{-2}$ with 95 % of FE towards CO, at a cell potential of -3 V using 1 M KOH as the electrolyte), as a result of the incorporation of multi-walled carbon nanotubes (MWCNTs) in the Ag catalyst layer of gas diffusion electrodes. The MWCNTs were helpful in reducing the charge transfer resistances of the electrode.[45] This catalyst is one of the most promising candidates illustrated in Fig. 6. Tornow *et al.*[46] studied the synthesis and application of carbon supported, nitrogen organometallic silver

View Article Online
DOI: 10.1039/C7GC00398F

catalysts with the aim of reducing CO_2 through the addition of an amine ligand to Ag/C. They found that 3,5-Diamino-1,2,4-triazole supported on carbon (AgDAT/C) produced about -70 mA·cm^{-2} of current density and almost 90 % of Faradaic efficiency for the production of CO. The use of a low Ag loading is another advantage of this study. Sastre *et al.*[26] have recently reported 10 to 40 wt% Ag nanoparticles supported on graphitic carbon nitride (g-C_3N_4). They reached a current density of up to about -20 mA·cm^{-2} (at -1.65 V *vs* SHE), and were able to change the CO/H_2 ratio from 100/1 to 2/1 by controlling the reaction parameters and the metal loading of the catalyst. The highest CO productivity (~ 60 mmol·cm^{-2}·h^{-1}) was achieved by using 40 wt% Ag loading at -1.15 V *vs* RHE.

Different reactors configurations have been used with Ag based catalysts. For instance, silver-coated ion-exchange membrane electrodes (solid polymer electrolyte, SPE) have been used at ambient pressure and temperature.[38] The result was 53 % of CO Faradaic efficiency with a high overpotential (2.43 V), but two side products of this reaction were HCOOH (formic acid) and H_2. Delacourt *et al.* [15] presented a new electrochemical cell configuration in which a pH buffer layer was used with the aim of adjusting the CO/H_2 ratio. They obtained a CO/H_2 ratio of 2/1 and a current density of 80 mA·cm-² at -3.5 V *vs* SHE, which, in principle, can be used for the production of methanol. However, a critical issue that emerged during the experiments was the change in the products selectivity after long-term co-electrolysis.[15]

Hara *et al.* [47] instead conducted high pressure experiments with Ag foil electrodes in 1997. In order to overcome the low solubility of CO_2 in aqueous electrolytes, they increased the pressure to 20 bar, and reached a current density of -300 mA·cm^{-2} with a Faradaic efficiency of 86 % towards CO.[47]

It can be observed, from data in Table S1 (*SI*) and Fig. 6, that the highest CO_2 current density achieved up to now, under atmospheric conditions, is of about -440 mA·cm^{-2} (exp. 22) by using a Ag-based gas diffusion electrode in a highly alkaline electrolyte (3M KOH) and that values close to 100 % of Faradic efficiency have also been obtained by employing ionic liquids as electrolytes (see exp. 19 and 21, in the absence of aqueous media), but the CO production has been negligible.

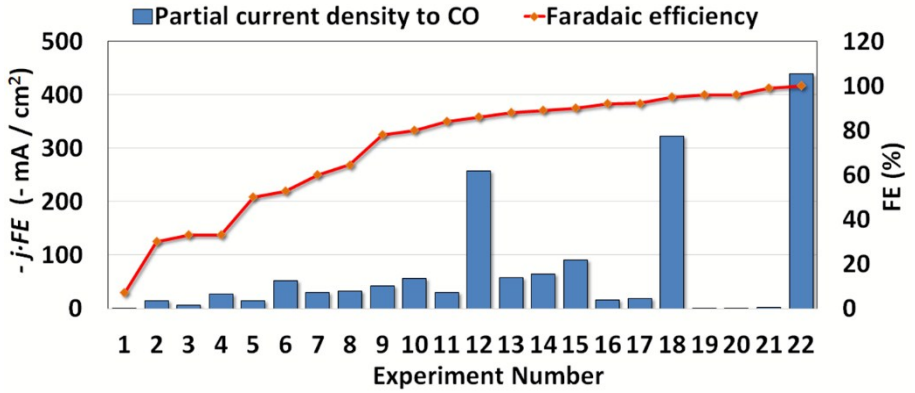

Figure 6. Current densities and Faradaic efficiencies related to CO production from the electrochemical reduction of CO_2 on Ag based electrodes. The experiments refer to the data in Table S1 (*SI*).

It is worth noting that a constant selectivity and a good stability have still not been demonstrated for most of the works reported in Table S1, since most of the electrodes were tested for no longer than 7 h, with the exception of the works conducted by Sastre *et al.*[26] and Liu *et. al.*[42], in which tests as long as 20h and 7 days were reported, respectively. Additionally, the scale-up of such electrodes has still not been achieved; most of the tests were performed with smaller electrodes than 6.25 cm^2. Hence,

View Article Online
DOI: 10.1039/C7GC00398F

the issue of a large (scaled-up), stable and continuous CO production (*i.e.* a fixed CO/H_2 production ratio) over long periods of times still remains a matter for technological research and development.

4.1.2. Au based electrodes

Among all the polycrystalline metals, gold exhibits the highest activity and selectivity for the reduction CO_2 to CO.[29] Recent advances in the synthesis of Au nanoparticles (NPs) have led to the synthesis of lower cost electrodes, which have also increased reaction rates, due to the control of both the surface area and the morphology of the active surface. Table S2 shows the details of the different experiments carried out with Au electrodes, and Fig. 7 illustrates the corresponding current densities and Faradaic efficiencies achieved for the CO production.

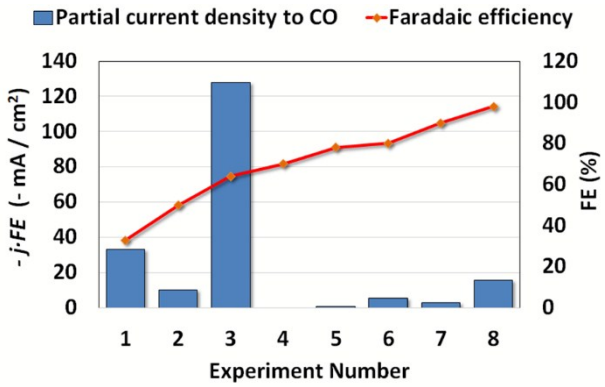

Figure 7. Current densities and Faradaic efficiencies related to the production of CO from the electrochemical reduction of CO_2 on Au based electrodes. The experiments refer to the data in Table S2 (*SI*).

One of the most promising aspects about the use of Au NPs has been their superior resistance to poisoning. This contamination is most likely causes by the electrodeposition of other metals, like Pt from the anodic counter electrode, which were found to influence the bonding energy of the CO on the cathodic electrode surface. Irreversibly adsorbed and bridge-bonded CO can poison the Au catalyst surface by blocking the catalytic sites, up to a surface coverage of ~0.2.[48,49] In the report by Chen and co-workers,[50] a significant improvement in longevity was observed with an Au NPs electrode, if compared with bulk gold, although they only tested the material for a maximum of 2h. Zhu *et al.*,[20] who considered different mono-disperse NPs (of 4, 6, 8, and 10 nm), showed that 8 nm Au NPs showed the maximum CO Faradaic efficiency (up to 90 % at -1.08 V vs. SHE) during the CO_2 electrolysis in 0.5 M $KHCO_3$ at 25 °C. Moreover, Au NPs embedded in an ionic liquid matrix of butyl-3-methylimidazolium hexafluorophosphate, which was employed for a more efficient COOH* stabilization, exhibited a good reaction activity per mass of active catalyst (~ -3 A/g of mass activity) and a notable selectivity (~ 97 % of FE) at -0.93 V *vs*. SHE, but with a low current density value of -3 $mA \cdot cm^{-2}$.[20] One of the lowest overpotentials (*i.e*. 140 mV, see Fig. 3) so far reported for the CO production has been achieved by Chen *et al.*,[50] who, using Au NPs, reached 78 % of FE, but with a low current density of -1 $mA \cdot cm^{-2}$. They reduced an Au oxide into Au particles with metastable surfaces that accelerated the CO_2 reduction catalysis by stabilizing the intermediates in the process. System stability was proved for a maximum of 8 h.

View Article Online
DOI: 10.1039/C7GC00398F

In a different reaction system, Delacourt *et al.* [27] studied Au plates and Au NPs dispersed in C-based supports as cathodic electrodes in a buffer layer BL-type cell, in which aqueous $KHCO_3$ was placed between the cathode catalyst layer and a proton-exchange-membrane (PEM). The highest current densities obtained with Au-based electrodes, namely 100 and 200 $mA{\cdot}cm^{-2}$, were achieved with those catalysts by controlling the thickness of the buffer layer.[27] Moreover, this system resulted in an adjustable Faradaic efficiency, as well as the best partial CO current density (~ - 128 $mA{\cdot}cm^{-2}$ with a FE of 64 %, see exp. 3 in Table S2, *SI*, and Fig. 7) so far reached with Au-based catalysts for the CO_2 reduction. Nevertheless, the long-term stability of such a system has still not been demonstrated.

4.1.3. Other systems

Owing to the high price and low abundance of noble metals, such as gold and silver, the use of other materials with comparable performance to Ag and Au has received increasing attention in recent years. Thus, a variety of more affordable non-noble metals, such as Cu, In, Bi, Mn, Fe, Mo, Ni, and Zn, among others, as well as other precious metals like Pd and Rh, have been screened as electrocatalysts for the reduction of CO_2. Table S3 (*SI*) summarize some of the best results reported in the literature for those electrocatalysts that have been tested for the CO production. As can also been observed in Fig. 3 and Fig. 8, the efficiency and CO production rate differ from one metal to another, because they depend on both the electrode properties and the reactor characteristics.

It is evident, from Fig. 8 that high current densities for the CO production (*i.e.* - 172.5 and - 99.4 $mA{\cdot}cm^{-2}$) have only been achieved only with other noble metals such as Pd and Rh, respectively, coupled with high pressure reactor systems. These results were obtained in an effort made by Hara *et al.* [47, 51] about 20 years ago, when they tested Co, Rh, Ni, Pd, and Pt electrocatalysts supported on gas diffusion electrodes (GDE) under high pressure (20 bar). They achieved an electrochemical reduction of CO_2 with a high performance, *i.e.* - 300 $mA{\cdot}cm^{-2}$ and almost 60 % FE for CO production.

As far as non-noble metals are concerned, the low cost and abundant copper (Cu) and Tin (Sn) catalysts have been shown to be highly active for the reduction of CO_2, but poorly selective for the production of CO, rather than for the production of methane or formic acid.[52, 53] Nevertheless, Zhao *et al.*[54] found that when 1-n-butyl-3-methylimidazolium hexafluorophosphate ($BmimPF_6$) was used as an ionic liquid solvent and electrolyte, supercritical (SC) CO_2 and water were electrocatalytically converted into a Cu cathodic electrode that produced CO, H_2, and a small amount of formic acid. By increasing the pressure up to 104 bar, they achieved up to 50 % of FE for CO and -20 $mA{\cdot}cm^{-2}$ of current density. It is worth mentioning the recent work by Kas *et. al.*[55] in which three dimensional porous hollow fibre Cu electrodes, used as both a gas diffuser and a cathode, has led to similar results to those achieved using noble metals, that is, a maximum FE of 75 % for CO at a potential of 0.4 V *vs* RHE and a current densities of up to - 17 $mA{\cdot}cm^{-2}$ at moderate potentials (- 0.3 to - 0.5V *vs* RHE). The good electrocatalytic performance of these electrodes was attributed to a defect-rich porous structure, in addition to a favourable mass transport conditions. In addition, Li *et. al.* [56] studied core/shell Cu/SnO_2 structures, where a thin layer of SnO_2 was coated over Cu nanoparticles, and the reduction of the CO_2 was found to be Sn-thickness dependent: the thicker (1.8 nm) shell showed Sn-like activity that resulted in the generation of formate, whereas the thinner (0.8 nm) shell was selective in the formation of CO, reaching 93 % of FE at - 0.7 V vs. RHE, but with low current density.

Bismuth has been observed to be a of the potential substitutes for the noble metals. For instance, Medina-Ramos *et. al.*[57] synthesized a Bi-based carbon monoxide evolving catalyst (Bi- CMEC) by means

View Article Online
DOI: 10.1039/C7GC00398F

of an electrodeposition method, and produced CO with 95 % of FE, but with a current density of -31 mA·cm^{-2} and a high over potential of about 1.23 V.

Some recent works have shown that the immobilization of a cobalt porphyrin onto a conducting diamond support,[58] or nickel onto a conducting poly(allylamine) support,[59] can promote the electrocatalytic production of CO. However, these heterogeneous architectures do not currently display technologically relevant current densities (fast kinetics) for CO_2 conversion applications.[57] In addition, with the current advances in homogenous catalysts for CO_2, very good results have been achieved for a system with Ni(cyclam)$^{2+}$ (cyclam = 1,4,8,11-tetraazacyclotetradecane)[60] and for an enzymic catalyst of Ni-CODH, in which microbial interconversions between CO and CO_2 were catalysed by carbon monoxide dehydrogenases (CODH).[61, 62] Although both of these systems achieved 100 % percent of FE with no overpotentials, the industrialization and commercialization of these processes are still important challenges.

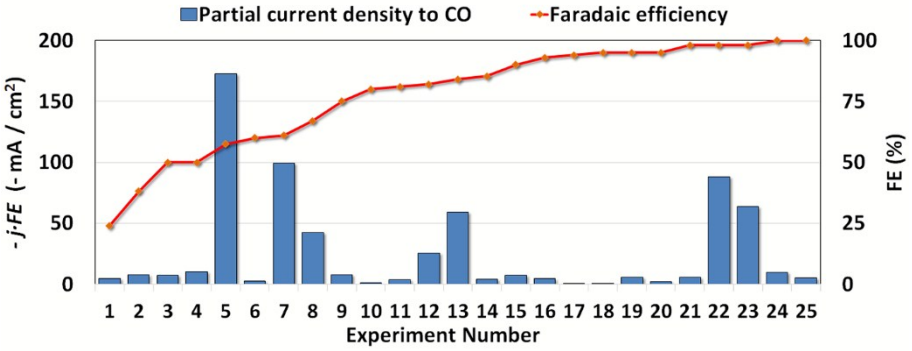

Figure 8. Faradaic efficiency and current density for the production of CO in systems that adopted different electrodes from Ag or Au. The experiments refer to the data in Table S3 in the *SI*.

4.2. H_2 Production

Since H_2 is produced during the reduction of CO_2 in aqueous media, it is essential to consider the kinetics of the HER to optimize the CO_2 conversion to syngas, and to be able to control the H_2/CO ratio. Therefore, a brief overview of the heterogeneous electro-catalysts that improve the reaction rate and efficiency of HER, and their optimum operative conditions is discussed hereafter (more details are in the supporting information, *SI*).

During the last few decade, several elements, such as Cu, Au, Pd, Rh, Fe and Mo,[63-65] Ni,[66-68] Ru,[69, 70] and Co,[71] have been investigated with the aim of finding a suitable replacement for Pt that would be the most active H_2 evolution catalysts. Because of the promising results that have recently been achieved, HER catalysts based on earth abundant elements, such as Co, Fe, and Ni, have been at the centre of the attention in current research.[71-77] The increase of the surface area of the cathode has been reported as a key parameter in the decrease of the HER overpotential.[32, 78] For instance, HER can be achieved under an aqueous buffer solution with neutral pH by using the recently proposed cobalt-oxo/hydroxo-phosphate catalyst developed by Cobo *et al.*[71] Other research works focussed on the use of metal alloys, such as CoMo, [32, 77] FeMo,[79] Ni-P graphite,[80] NiFeMo or NiMo, [81] which have evidenced both good corrosion resistance and good HER activity For instance, Arul Raj et. al.[81] have reached HER at -0.187 V of overpotential, by using NiFeMo and NiMo cathodes, over 1500 h of continuous electrolysis under typical industrial conditions. McCrory *et al.*,[32] in a recent study, have benchmarked 18 HER electro-catalysts using a standardized protocol to evaluate their activity under acid (1M H_2SO_4)

View Article Online
DOI: 10.1039/C7GC00398F

or basic conditions (1M NaOH). As shown in Fig. 9, they tested several non-noble metal based HER catalysts that can operate at -10 mA·cm^{-2} with overpotentials < 0.1 V in acidic and/or alkaline solutions.

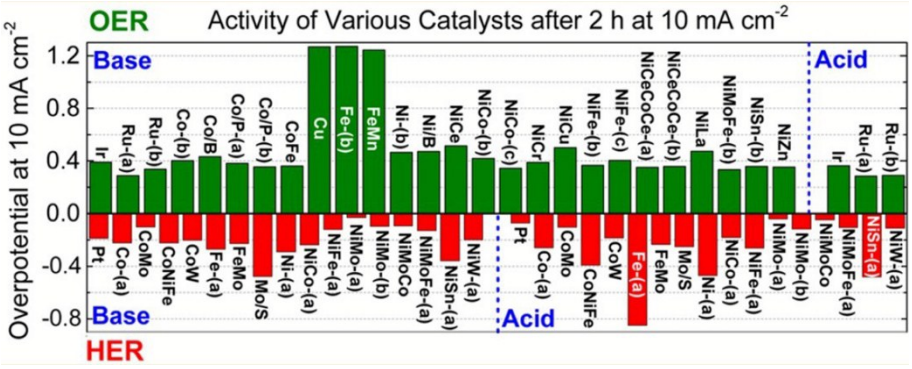

Figure 9: Benchmarking of Hydrogen Evolving Reaction and Oxygen Evolving Reaction Electro-catalysts. Reprinted with permission from [32] with the kind permission of the. Copyrights 2015.

In particular, the effect of pH on noble-metal catalysis is currently a topic of vigorous scientific discussion.[66, 82] Electro-catalysis of HER in acid and alkaline media, by means of Cu, Ag, Au, Pt, Ru, Ir and Ti electrodes, has been described by Danilevoc *et al.*[82] Because of coverage by spectator species, even in the HER potential region, the authors questioned whether it would be possible to experimentally establish a true/real relationships between M–H_{ad} (M: Cu, Ag, Au, Pt, Ru, Ir and Ti; H_{ad}: adsorbed H_2) energetics and catalytic activity. In fact, with the exception of Pt, Ir and Au, the experimentally established positions of the other metal catalysts in the observed volcano relationships were found to be uncertain over the entire pH range.

Among the noble-metals that are less expensive than Pt, Au is considered one of the most favourable candidates for HER, because it is catalytically active (also in the form of bimetallic surfaces, e.g. Au/Pd)[83] and is rather stable.[8, 84-89] The knowledge of HER on Au electrodes is quite important for the electrocatalytic production of syngas because Au is also one of the most promising electrocatalysts for the reduction of CO_2 to CO. The kinetics of hydrogen evolution on electro-deposited Au electrodes have showed polarization curves consisting of two linear segments: [90] the kinetics in the higher-slope region (at high current densities and overpotentials) depends on the composition of the solution (pH, ionic strength), while the overpotential did not depend on the pH or ψ_1-potential in the lower slope region. This finding is in accordance with the barrierless discharge theory (*i.e.* the lack of the presence of an activation barrier over the final state of discharge, *i.e.* adsorbed H atom) of H_3O^+ on a gold electrode, which was to have been expected since gold poorly adsorbes H_2,[90] and could be exploited to control the H_2/CO ratio in Au-based electrocatalytic systems.

5. Factors that influence the CO_2 reduction to CO process

Several factors are known to affect the efficiency of the CO_2 reduction process. The strategies employed to enhance this process are based on varying one or several of these factors. Nevertheless, the advantage of using a particular combination of several design options (*i.e.* reactor configuration, electrode material, electrolyte, pressure, temperature, *etc.*) is not clear in much of the literature. Moreover, the products analysis is not always complete, and thus the Faradic efficiency and the exact composition of the product stream cannot be readily known.

5.1. Electrochemical reactor configuration

View Article Online
DOI: 10.1039/C7GC00398F

The choice of reactor device has profound effect on the efficiency of the CO_2 electrocatalytic reduction. Furthermore, the fact that there is no standardized method or well-established protocol for this process makes it more difficult to make a comparison between the different experiments in different labs. The main challenge is to achieve the CO_2 conversion with the lowest overpotential and with a competitive energy efficiency.

Different types of electro-catalytic reactors have been used, but only the most promising concepts from the literature are discussed hereafter. Fig. 10 summarizes the different reactor configurations. The design of photo-electro-chemical (PEC) cells that combine both solar water oxidation and CO_2 reduction in a monolithic reactor have not been dealt with in detail as these types of systems have recently been discussed in other works.[25]

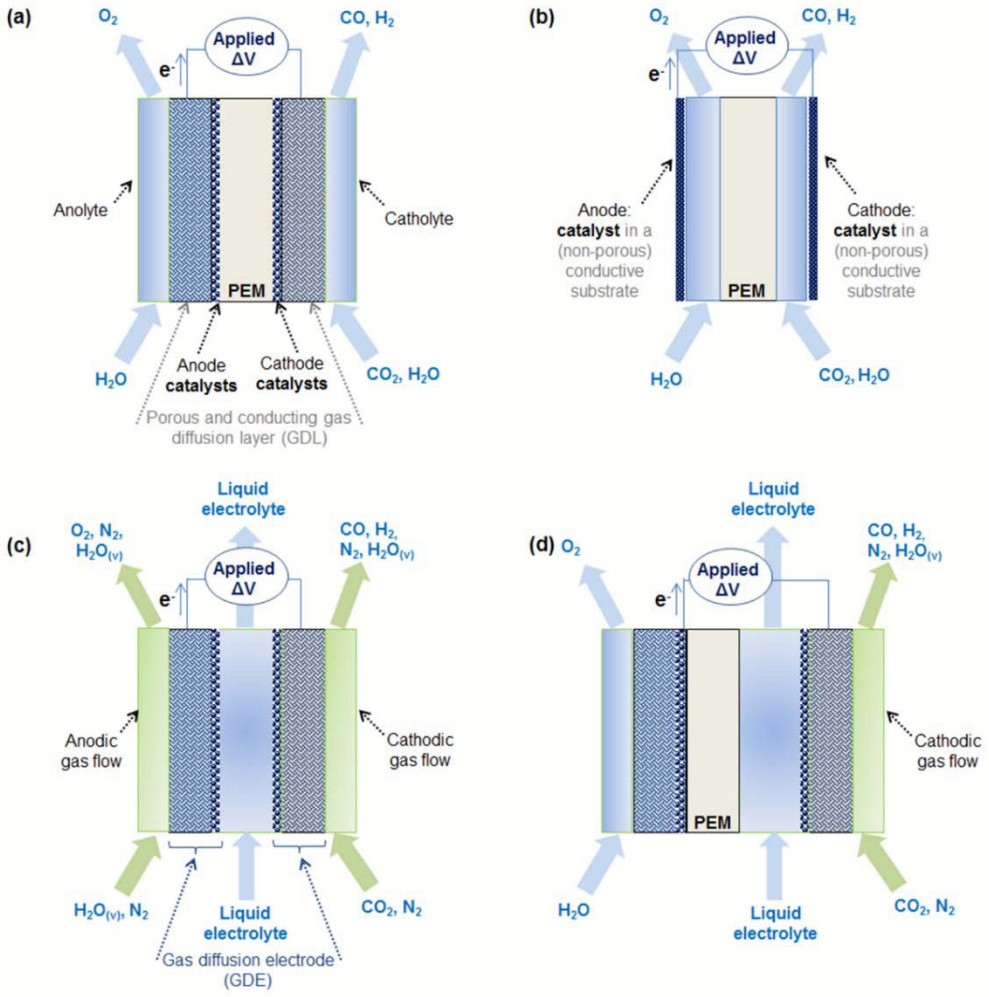

Figure 10. Schematic representation of different electrochemical reactors used for the reduction of CO_2 to CO: (a) the anode and cathode catalysts are supported on microporous gas diffusion layers (GDLs) and are separated by a PEM; (b) the anode and cathode catalyst are supported on conductive non-porous substrates and are separated by both a PEM and two layers containing the anodic and cathodic liquid electrolytes; (c) the anode and cathode catalyst are both supported on GDL and constituted by gas-diffusion electrodes, which are fed by gas streams on the non-catalytic side, and are separated by a stream of liquid electrolyte in contact with the catalytic sides; (d) like (a), but this time the cathode is a gas diffusion electrode fed by a gaseous CO_2-containing stream, and its catalytic side is separated from the PEM by a liquid buffer layer. PEM: polymeric (ion) exchange membrane; GDL: gas diffusion layer (conductive and permeable to water). The cathodic outlet could

View Article Online
DOI: 10.1039/C7GC00398F

contain not only CO, but also other CO_2 reduction side products, which have not been indicated here for the sake of brevity.

One of the most frequently used configurations is a two compartments cell that employs a PEM to separate the anode and cathode electrodes in order to prevent the anolyte and catholyte solutions from mixing (Fig. 10a), in a similar way to PEM fuel cells. In this kind of reactor, the catalysts can be deposited directly onto the PEM,[38] or they can be coated on the gas diffusion layer (GDL) substrates that are water/gas permeable and conductive. The thus formed electrodes, are then hot-pressed with the PEM in order to enhance the mass transfer at the catalyst-membrane interphase.[91] The simultaneous requirements of selective ion transport through the membrane (to maintain the pH solution constant on both sides),[92] and inhibition of the product crossover constitute significant constraints for these systems.[93]

Cation exchange membranes (CEM) that are proton conductive (*e.g*. Nafion) are frequently employed, and as a result, the H^+ produced by the oxygen evolution reaction or cations (*e.g.* K^+) present in the anolyte can diffuse from the anodic to the cathodic chamber. If a CEM is used, the anode must/should operate in acid, which/and this requires the use of oxygen evolution catalysts based on expensive noble-metals (*i.e.* Ir, Ru). In fact, as shown in Fig. 9, no other kind of electrode is able to achieve the oxygen evolution reaction (OER) with a low overvoltage and to attain good stability.[32]

Research has been conducted in which AEM has been employed to allow the OH^-, HCO_3^- and CO_3^{2-} ions to diffuse, above all when basic electrolytes (*e.g*. bicarbonate) are used in the cathodic chamber.[38] The use of AEM usually results in a less efficient anode performance, and increases the rate of crossover products, especially of neutral and anionic products, such as methanol and formate, from the cathode to the anode.[93]

As proposed by Hori et al.,[38] the difference between the use of AEM and CEM in a quasi-neutral solution (e.g. K_2SO_4), may be rationalized as follows: OH^- is generated at the electrode during the cathodic reduction of CO_2 in aqueous media.

$$CO_2 + H_2O \quad + 2e^- \rightarrow CO + 2OH^- \qquad (5)$$

The resultant OH^- will react with the dissolved CO_2 and form HCO_3^- or CO_3^{2-}. In the presence of K^+ ions, $KHCO_3$ or K_2CO_3 is formed at the metal-membrane interface. However, neither OH^-, HCO_3^- nor CO_3^{2-} can be eliminated from the metal-membrane interface in a CEM. Thus, K_2CO_3 is accumulated and flows out from the electrode, and as a result the metal peels from the membrane or deactivates the catalysts surface. In another cases, if the metal-membrane interphase is highly acidic (*e.g*. when Nafion is used), the CO_2 conversion reaction could be suppressed, due to the prevalence of the more favourable H_2 evolution reaction. On the other hand, both OH^- and CO_3^{2-} can easily be eliminated from the metal-membrane interface on an AEM due to their mobility within the membrane and, as a result, the CO_2 reduction reaction is favoured.

A more traditional reactor configuration, which is commonly used for screening experiments, is represented in Fig. 10b. This configuration is a two-compartment cell divided by a PEM, in which the catalytic surface of the anode and cathode electrodes are immersed in liquid electrolytes. This kind of system is used to test the electroactive surfaces of catalysts supported on non-porous or water permeable materials. An example of this kind of system is the electrochemical reactor introduced by Jaramillo and co-workers, shown in Fig. 11a,[94, 95] which is characterized by a geometry that maximizes the cathode exposed area *vs* the catholyte volume, *i.e.* 4.5 cm^2 *vs* 8 ml, and is thus able to optimize

View Article Online
DOI: 10.1039/C7GC00398F

the efficiency of the reactor by minimizing the ohmic losses. With such a system, Hatsukade *et al.* were able to identify and quantify, with a high sensitivity, six CO_2 reduction products, including CO and hydrogen as the main products, and formate, methane, methanol and ethanol as minor products, on a metallic silver surface (see Fig. 11b). In addition, they measured a CO_2 reaction rate *vs* potential profile (Fig. 11c), and correlated it with the CO productivity, demonstrating that the reaction at potentials more negative than - 1.1 V *vs* RHE is limited by mass transport (of CO_2 to the catalyst surface) rather than by kinetic control. Such a result encourages future work on the development of electrochemical reactors with better mass transport properties to extract the actual kinetic values at high overpotentials.

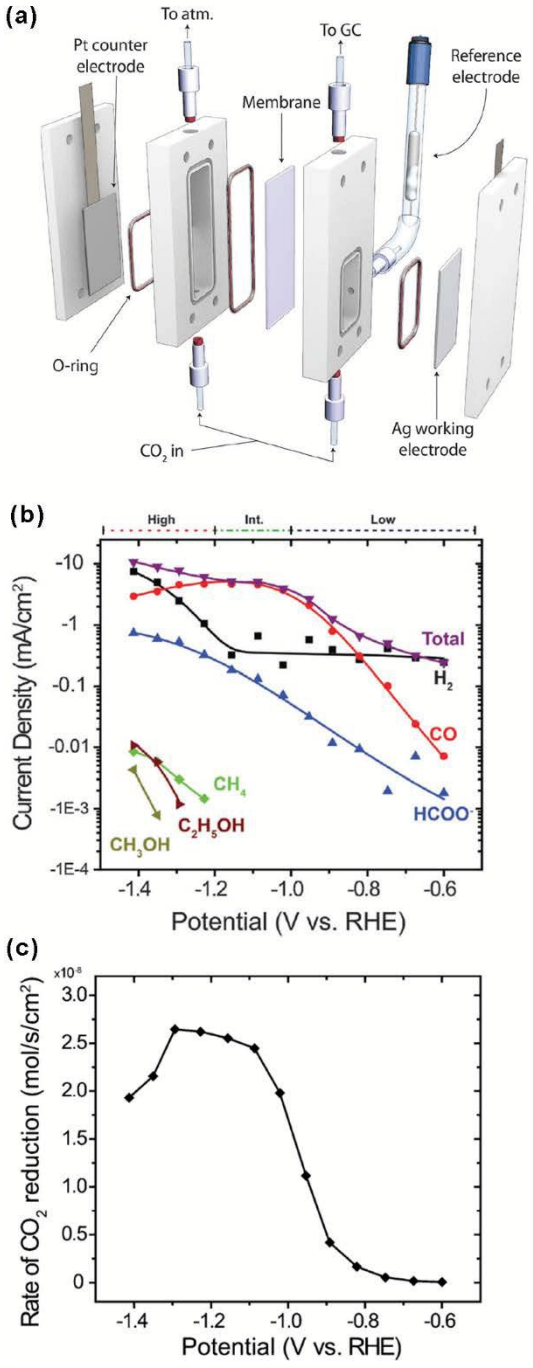

Figure 11. a) A schematic view of the electrochemical cell reported by Jaramillo and co-workers, b) Tafel plot of the partial current density of each product of the CO_2 reduction on an Ag surface and c)

Total rate of CO_2 reduction rate as a function of the potential. Reproduced and adapted from [95] with the kind permission of the PCCP Owner Societies.

Another versatile reactor system, of the same kind as that shown in Fig. 10b, is the one developed by Satre *et al*.,[26] shown in Fig. 12, in which parameters, such as the amount of CO_2 dissolved in the liquid phase, temperature (5 - 100 °C), pressure (1 - 8 bar) and applied potential *vs* a reference electrode, can be controlled. The difference from the reactor in Fig. 11a is that, in this case, the electrodes are completely immersed in the electrolyte solutions, and in this way both sides can take part in the catalytic reaction. Moreover, although the distance between the electrodes (and consequently the ohmic drop) has not been optimized, this reactor can work in either batch or continuous mode operation.

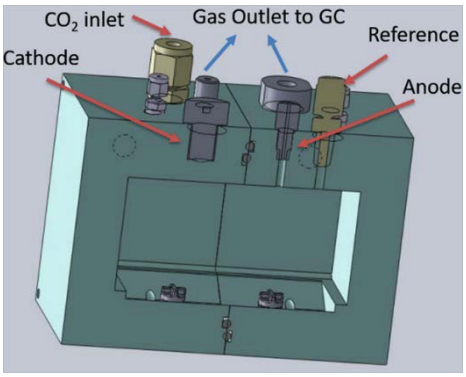

Figure 92. A schematic view of the electrochemical cell reported by Sastre et al. Reprinted from [26] with the kind permission of John Willey and Sons. Copyright 2016.

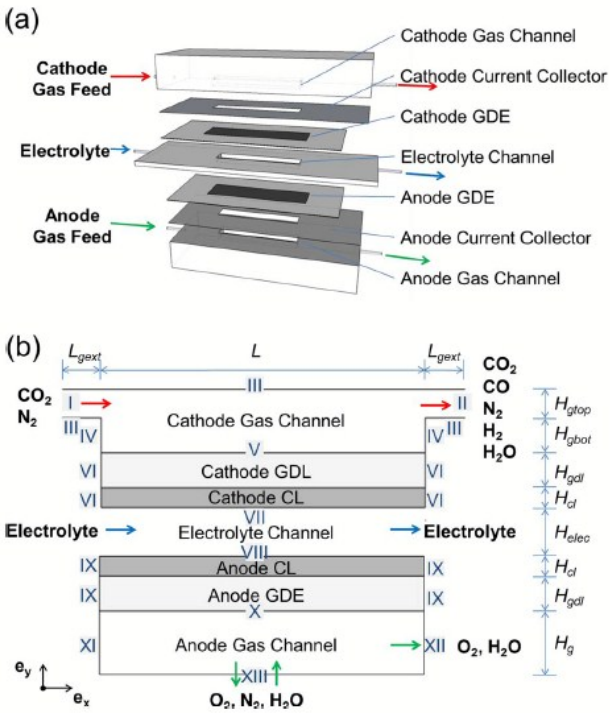

Figure 103. A schematic view of the microfluidic cell reported by Wu *et al.* for a CO_2 reduction to CO with details of: a) various functional layers and b) a simplified schematic used for modelling. Reproduced from [96] with the kind permission of The Electrochemical Society. Copyright 2014.

View Article Online
DOI: 10.1039/C7GC00398F

In order to address the issues coming from the use of cationic or anionic PEM, different structures have been developed and are represented in Fig. 10c and 10d.

The configuration shown in Fig. 10c represents a novel kind of reactor that was introduced by Kenis *et al.*[96, 97] and which is shown in Fig. 13. This reactor exploits electrocatalysts supported on GDLs, that is, the so-called gas-diffusion electrodes (GDEs). This kind of reactor directly introduces gaseous CO_2 as a reactant onto the cathode surface, and offers the advantage of increasing selectivity towards CO_2 conversion. The versatile microfluidic reactor that they developed was based on several parallel layers, and it used anode and cathode GDEs, with an aqueous electrolyte channel between the anode and the cathode electroactive surfaces (see Fig. 13). In addition, a steady-state isothermal model, which integrates the transport of the charge, mass and momentum with electrochemistry for both the cathode and anode, was proposed in their work for the electrochemical reduction of CO_2 to CO. The main advantages of such a system is that several operating parameters, such as the applied cell potential, the CO_2 concentration of the feed and the feed flow rates, as well as the reactor design parameters, such as channel length and porosity of the gas diffusion electrodes, can be varied and systematically studied to determine their influence on the selectivity and productivity for CO and H_2 (syngas) production.

Another application to a cathodic gas-diffusion electrode (GDE), which is schematised in Fig. 10d, was proposed by Delacourt *et al.*[15, 27] and by Dufek *et al.*[98, 99] Such systems exploit a liquid electrolyte between the cathode catalytic side and the PEM. In general, noble-metal based anodes (*i.e.* Ru, Ir, Pt) are assembled in a CEM. The advantage of this kind of system is that it offers the possibility of controlling the H_2/CO ratio by reducing the amount of H^+ that reaches the cathode, as a way of achieving a lower H_2 evolution. This can be obtained by using a bicarbonate buffer layer as a catholyte, as shown in Fig. 14a, or by varying the CO_2 flow rate, as will be explained in more detail in the next sections.

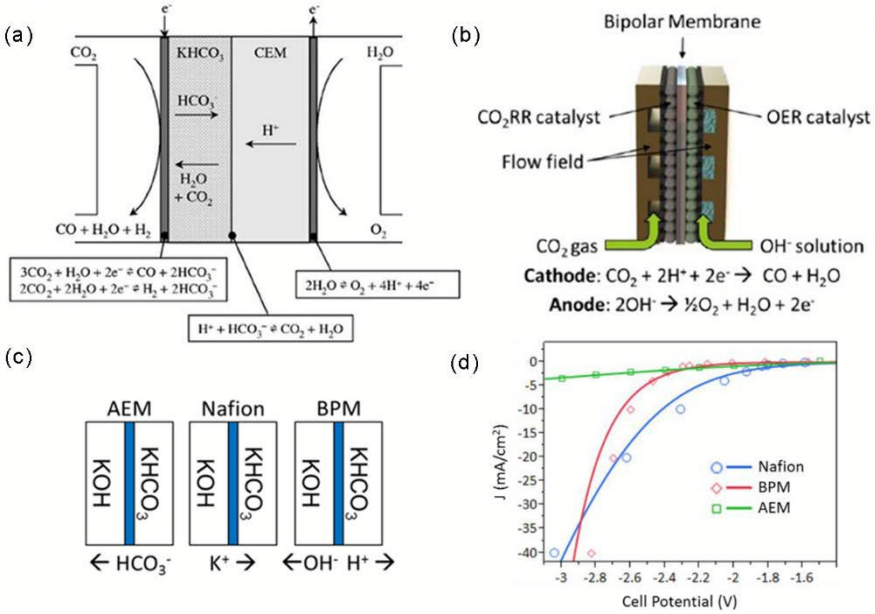

Figure 14. CO_2 reduction cells for syngas production based on GDE: (a) schematic of the buffer layer-type electrolysis cell by Delacourt *et al.* [15, 27]. Reprinted from Ref. [27] with the kind permission of The Electrochemical Society. Copyrights 2010. (b) Schematic drawing of the gas-fed CO_2 electrolyzer by Li et al. [93]; (c) illustration of the predominant ion transport processes during electrolyzer operation with AEM, Nafion, and bipolar membranes; (d) j–V curves for a BiOx/BMIM$^+$OTf$^-$-catalysed GDE-

View Article Online
DOI: 10.1039/C7GC00398F

based cell compared to BPM, AEM, and CEM membranes. Adapted from [15, 27, 93] with the kind permission of the American Chemical Society. Copyrights 2016.

Over the last two years, bipolar membranes (BPM) have been coupled with CO_2 reduction catalysts supported on GDL (Fig. 10a), or working as GDEs (Fig. 10d), in order to exploit innovative solutions that combine the most promising approaches. BPMs, which are generally used more for the production of acids and bases, consists of an anion and a cation exchange membranes that are laminated together, often with a catalyst that promotes the auto-dissociation of water at the interface. Thus, in the applied electric field, the hydroxide ions and protons produced in the bipolar junction move towards the respective electrode.[93, 100] In the work by Li et al.,[93] a CO_2 electrolyzer system, based on a commercial BPM with an alkaline NiFeOx OER catalyst, was studied with both Ag/aqueous bicarbonate (as in Fig. 10a) and BiOx/ionic liquid/gas-phase CO_2 catalyst/catholyte compositions (see Fig. 14b). The Ag catalyst had a CO_2 reduction onset potential of −1.05 V *vs* Ag/AgCl in aqueous $KHCO_3$, and a current density of -30 $mA{\cdot}cm^{-2}$ at −1.5 V. They compared the performance of a BPM (Fumasep) with that of two commercially available membranes, that is, a CEM (Nafion) and an AEM (Neosepta). A shift of -0.6 V of the onset potential of the AEM and CEM was observed when using BPM was used (from -1.6 V to -2.2 V), due to the additional thermodynamic driving force required by the cell for acid−base neutralization reactions, and a loss of ∼300 mV occurred in the BPM cell because of the reaction of protons with HCO_3^- ions.[93] However, the Nafion-based cell did not remain stable in the long-term, because the anolyte and catholyte pH progressively became more acidic and basic, respectively. On the contrary, the dissociation of water in the BPM-based cell drove the H^+ and OH^- ions towards the cathode and anode, respectively; the pH of the anode and cathode remained constant, and as a result, high current densities and stable operation were achieved for the production of CO + H_2 mixtures in the BPM-based cells. Fig. 14d shows the j−V curves of the cells gas-fed with AEM, Nafion and BPM, operating with earth-abundant and low-cost BiO_x catalysts on carbon paper drop-coated with an ionic liquid (*i.e*. $BMIM^+OTf^-$) as the co-catalyst to stabilize the CO_2^- intermediate. This system operated stably for 14 h, without any loss of activity at -80 $mAcm^{-2}$, with a cell potential of about 3 V. However, the CO FE deteriorated within 1 h, probably due to de-wetting of the ionic liquid from the catalyst surface.[93]

It is worth noting that all of these types of configurations were developed at a laboratory bench-scale. However, it is clear that a reactor scale-up is necessary to implant this technology in an economically viable industrial process. Only a few papers that have dealt with this issue. The scale-up of these configurations currently represents an interesting engineering challenge. For instance, although not for the CO generation, Oloman *et al.*[101] reported a scale-up from 45 to 320 cm^2 of the cathodic area, although not for CO generation, and they achieved analogous performances for formate production from CO_2. They reached current densities of between 0.6 and 3.1 kA m^{-2}, with a cell voltage of -2.70 to - 4.45 V and formate production efficiencies of between 63 and 91 %, respectively.

5.2. Approaches adopted to control of the H_2/CO ratio

The best way of achieving a highly sustainable CO_2 reduction process is through the use of a renewable power source and the control of the electrochemical reaction products. In this way, if the produced stream has a controlled composition (H_2, CO and side products), it can be used directly in another reactor to produce a higher added-value product (fuels or fine chemicals), thus avoiding the use of separation equipment, which would increase both the operational and investment costs of the process.

View Article Online
DOI: 10.1039/C7GC00398F

As mentioned above, depending on the H_2/CO ratio of syngas it can be used in a different transformation process to obtain one of several products (see Fig. 2). This ratio generally depends on a variety of parameters, such as current density (applied potential), electrolyte feed rate, pH, temperature and, in some cases, on the catalysts composition or particles size. Therefore, although the optimization of the CO_2 conversion system is relatively complex, the development of electrochemical reactors that are able to produce a steady fixed syngas composition over time is of primary importance, because of the necessity of their easy and fast implementation and integration on existing infrastructures.[15] However, only a few works that have systematically studied the conditions necessary to obtain different H_2/CO ratios at steady state conditions, during the electrochemical reduction of CO_2.

Hori *et al.*[38] developed a PEM-based electrode in which silver was deposited directly onto ion exchange membranes (configuration shown in Fig. 10a, but without a GDL). The PEM electrodes made with an anion exchange membrane (AEM) were able to reduce CO_2 to CO for about 2 h, with -5 mA·cm^{-2} to - 60 mA·cm^{-2} of partial current density and a CO/H_2 ratio of 30 to 1.33, respectively. The transport of electrons and CO_2 to the electrode surface was enhanced on the AEM when this porous metal layer was used because of its high anionic conductivity. OH^- and CO_3^{2-} were easily eliminated from the metal membrane interface and permeated through the membrane to the electrolyte solution. Thus, the reduction of CO_2 was not prevented when an AEM electrode was adopted, as instead happened when a CEM was used[102] and could be sustained for a long time (~ 2h). In such a way, it was possible to control and maintain a fixed ratio between the H_2 and CO products in the system.

Delacourt *et al.* [27] proposed a system to reduce the gas-phase CO_2. This system uses an aqueous buffer layer (BL) of potassium bicarbonate between a CEM and a gas diffusion cathode (see Fig.s 10d and 14), and it was tested considering 3 different cathodic catalysts on GDEs: unsupported Au, Au supported on Vulcan carbon, and unsupported Ag. Since the pH at the cathode is not acidic, the electrochemical reactions of H_2 and CO evolution took place with a proton donor, *i.e.* H_2O or HCO_3^- rather than H^+. This system has the advantage of being independent of the proton donor or the form of CO_2 that is reduced, because the protons coming from the anode react with the bicarbonate ions.[15] This buffer layer is likely to probably prevents an excessive number of protons from reaching the cathode, so that only hydrogen evolved. Thus, if the thickness of this layer is to be changed, it could be used as a mass transfer barrier that could be controlled to tune the final desired product. The authors achieved ca. -30 mA·cm^{-2} with a potential of −1.7 to −1.75 V *vs* SCE (saturated-calomel reference electrode). A H_2/CO ratio of 2, which is suitable for methanol synthesis, was obtained at a potential of ca. −2 V vs. SCE and for a total current density of ca. -80 mA·cm^{-2}. The drawbacks of such a system are that, while this arrangement enabled the cell to operate stably, a Pt−Ir OER catalyst was used to ensure anode stability and a low overpotential in the acidic anolyte, and a free-energy loss was also observed associated with the acid−base neutralization reaction of H^+ and HCO_3^- at the interface between the CEM and the buffer layer.[93] In addition, another issue that was identified concerns the change in product selectivity after long-term electrolysis.

Mistry *et. al*.[103] reported the size-dependent catalytic activity of micelle-synthesized Au nanoparticles (NPs) for the CO_2 reduction to CO, and its effect on manipulating the H_2/CO ratio in the products. A drastic increase in current density was observed as the NPs size decreased, along with a decrease in the Faradaic selectivity towards the CO. On the basis of DFT calculations, the authors concluded that the trends were related to the increase in the number of low-coordinated sites on small NPs, which favoured the evolution of H_2 over the reduction of CO_2 to CO.

View Article Online
DOI: 10.1039/C7GC00398F

Liu *et. al*. [104] were also able to manipulate the H_2/CO ratio from 0 to 103 thorugh different approaches, such as varying the cell potential, changing the Ni/Ag loading of their electrocatalyst from 1/0 to 4/1 and increasing the acidity of the electrolyte. They obtained 99.1 % of selectivity by using the EMIM-Cl ionic liquid at pH 6.6, which shifted to 0.9 % when the pH was reduced to 0.5. They also observed remarkable current densities of up to -60 mA·cm^{-2} by using a solid electrolyte cell (such as the one in Fig. 10a, but with a humid CO_2 gaseous stream fed to the cathode chamber).

5.3. Electrolytes

The use of a liquid electrolyte in at least one part of the cathodic electrode is frequently adopted, and this adds complexity to the system. Different electrolytes, ranging from basic to acidic, have been studied extensively.[105, 106] Aqueous electrolytes, which are generally composed of alkali cations (*e.g*. Na^+, K^+), various anions, such as halide anions, bicarbonate (HCO_3^-) or hydroxide (OH^-), are employed for the heterogeneous electrochemical reduction of CO_2, due to their high conductivity in water. Water itself can be a source of proton exchange.[107] Hence, the employed electrolyte plays a key role in the production and selectivity of different products. This is why, the selection of the electrolyte can have a profound effect on the current density and selectivity of the CO_2 reduction products.

Hori *et al.*[108] studied the distribution of products obtained from the reduction of CO_2 in different electrolytes. They found a marked dependency of the availability of hydrogen or protons on the surface and the distribution of products for Cu electrodes. The pH at the electrode is affected by the electrolyte.[108] In other words, it is important to consider the pH and CO_2 concentration on the surface of an electrode during hydrogen evolution and CO_2 reduction, depending on the reaction (see Table 1) and on the production of OH^- ions or the consumption of H^+, the pH could increase. Moreover, the main problem arises from the fact that CO_2 acts as both a reactant and a buffer. The main equilibrium reactions in a bicarbonate CO_2 solution are:[109]

$$CO_2 + H_2O \leftrightarrow H_2CO_3 \leftrightarrow H^+ + HCO_3^- \quad pK_a=6.4 \qquad (6)$$

$$HCO_3^- \leftrightarrow H^+ + CO_3^{2-} \quad pK_a=10.3 \qquad (7)$$

As a result of the reaction (6), the pH varies from 6 to 8 (depending on the concentration of the bicarbonate) and because of the kinetics of the reaction (6) necessary for H_2CO_3 to be formed. Thus, most of the buffer capacity near the electrode surface where hydroxide forms results from reaction (1), and also from the direct reaction of CO_2 with hydroxide ions as follows:

$$CO_{2(aq)} + OH^- \leftrightarrow HCO_3^- \qquad (8)$$

These reactions will therefore result in higher local pH. Gupta *et al.*[110] have calculated these changes in local pH for Cu electrodes, and the results are shown in Fig. 15. As can be seen, most of the measurements were conducted with a pH of around 9. However, when the pH was increased to 10, the current density increased. It is likely that this increase in pH at high overpotentials suppresses HER. The decreased local concentration of CO_2 also caused a decrease in the CO production and an increase in methane and ethane production.[109]

The cations species also play an important role.[111] Wu et al. [112] observed different selectivities of Sn electrodes when they used different electrolytes (*i.e.* $KHCO_3$, K_2SO_4, KCl, Na_2SO_4, Cs_2SO_4, $NaHCO_3$, and $CsHCO_3$). Moreover, Kenis *et al.*[111] reported that the size of the cation ($Na^+ < K^+ < Rb^+ < Cs^+$) of the salt used in the electrolyte plays a significant role in the reduction of CO_2 on Ag electrodes. They in particular noted that larger cations favoured CO production and suppressed the evolution of H_2.

View Article Online
DOI: 10.1039/C7GC00398F

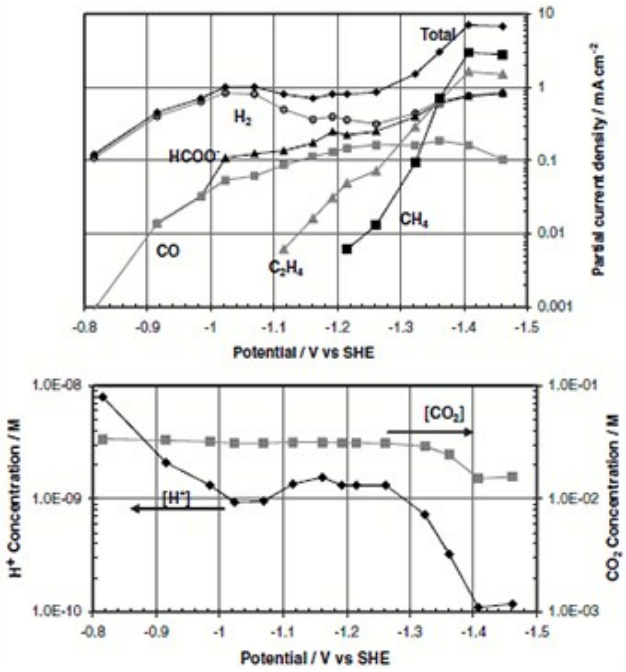

Figure 115. Partial current data from Hori *et al*.[108] (Conditions: 0.1M $KHCO_3$, 19 °C, CO_2 bubbled, bulk $[H^+] = 1.55 \cdot 10^{-7}$ M, bulk $[CO_2] = 3.41 \cdot 10^{-2}$ M. Estimated local $[H^+]$ and $[CO_2]$ values for polarization measurements from [110]. Reprinted and adapted from [109] with the kind permission of Elsevier. Copyright 2006.

Unlike the conclusions that were reached in the above mentioned works, in some recent works, the effect of alkaline electrolytes has shown to be in favour of CO production.[113-115] In an interesting work, Verma *et. al.*[114] have recently investigated the effect of different potassium salts (*i.e.* KOH, KCl, $KHCO_3$ at different concentrations) on the electrochemical reduction of CO_2 to CO on Ag-based GDE. They found that using a highly alkaline electrolyte (3M KOH) was better to reach very high current densities (*i.e.* -440 $mA \cdot cm^{-2}$) than the other considered electrolytes. This effect can be attributed to an improved stabilization of the $CO_2^{\bullet -}$ radical intermediate by a higher concentration of K^+ ions in the outer Helmholtz plane (OHP) of the electrical double layer. Higher concentrations of K^+ and OH^- will lead to a more compact double layer at the electrode-electrolyte interface, which in turn results in a shorter Debye length or an OHP closer to the electrode surface (see Fig .16).[21] They also concluded that when KOH is used as the electrolyte, the OH^- generated at the cathode has a greater chance to get consumed at the anode for the O_2 evolution reaction, and the continuous removal of the OH^- species from the cathode can enhance CO_2 reduction.[114]

View Article Online
DOI: 10.1039/C7GC00398F

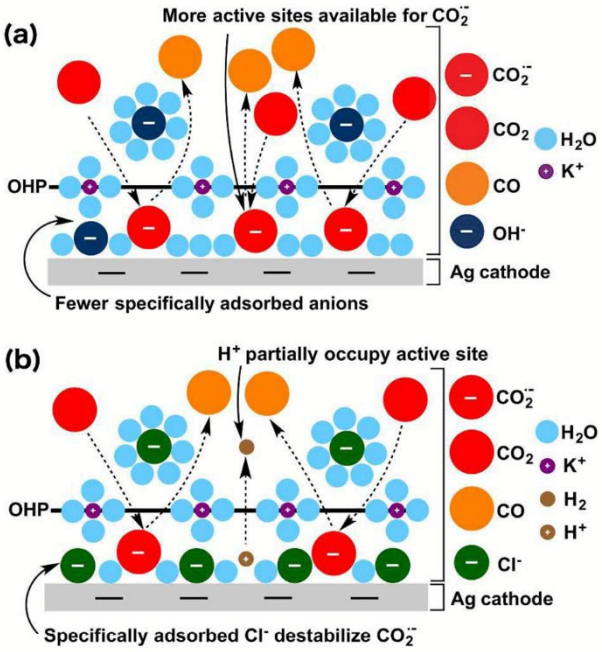

Figure 126. Schematic illustrations of processes in the double layer that play a role in the kinetics of CO_2 to CO conversion on a Ag cathode when using (a) KOH or (b) KCl as the electrolyte. Reproduced and adapted from [114] with the kind permission of the PCCP Owner Societies.

Ionic liquids, which have been reported by different research groups are also used as electrolytes, although this use is less common because they are expensive and sensitive to moisture. Kenis *et al*. [116] tested silver nanoparticle as a cathode, dried EMIM-BF_4 as a catholyte, and 0.5 M sulfuric acid as an anolyte. They have recently reported a selective conversion, with a low overpotential, using 18 mol% WMIN-BF_4 in water in the cathodic compartment and 100 mM aqueous sulfuric acid in the anode compartment.[117] They were able to reduce the formation potential of CO to 1.5 V. In addition, Salehi-Khojin *et al.*[118] studied the molybdenum bisulphite as cathode in an ionic liquid for the selective production of CO. They used 4 mol% EMIN-BF_4 in water (pH=4) for both compartments. The current density was as high as -65 $mA{\cdot}cm^{-2}$ for a low potential - 0.764 V, and 98 % of Faradaic efficiency towards CO production was achieved. Deng *et al.* [119] used an aqueous solution of 1-butyl-3-methylimidazoliumchloride (BMIM-Cl) with 20 wt.% H_2O and Ag metal as a cathode. They studied the selectivity impact of the products while varying the pH of BMIM-Cl with different H_2O concentrations. Verma et. al. [114] also studied mixtures of KCl with EMIM Cl, Choline Cl and their deep eutectic solvents, which are able to enhance the amount of CO_2 absorbed by the electrolyte. This led to a higher current densities for the CO production in comparison to aqueous solutions of these ionic liquids without KCl. Hence, electrolyte mixtures containing ionic liquids are promising as a strategy to integrate the processes of CO_2 capture with CO_2 conversion.

5.4. Temperature

In most of the above reported papers, the experiments were conducted at room temperature and ambient pressure. Nonetheless, commercial electrolyzers generally operate at 80-150 °C, because their temperatures normally increase due the heat that is generated to attain the exothermic reactions during operation. Hence, the effect of the temperature on the reduction performance of CO_2 and product distribution is very important. Dufek *et al.*[99] have recently studied a syngas production cell based on a GDE containing an Ag catalyst and a Ru-based anode, operating under different CO_2 flows, current densities and temperature conditions. They observed a monotonic drop

in the cathodic overpotential of up to 0.32 V at -70 mA·cm^{-2} as the temperature was increased from 18 °C to 70 °C. However, the overall cell potential dropped by 1.57 V, which could be attributed to several contributions. Firstly, the thermodynamic and kinetic parameters both influence the cathode potential for the H_2 and CO evolution reactions. It was calculated that the thermodynamic change in the reduction potential for both CO_2 and H_2O, as the temperature was increased from 25 to 125 °C, was less than 0.1 V.[99] This indicates that thermodynamics can only account for a portion on the observed reduction of the overpotential, and suggests that the main effect of the temperature increase is on the kinetics at the catalyst surfaces. Secondly, the remaining part of the drop in cell potential could be due to a decrease in the anode potential and a drop in the ohmic resistances of the electrolyte and membrane. The electrolyte conductivity should increase as the temperature increases and the produced gas bubbles become smaller, and this leads to a lower shielding effect of the electrodes and to better contact with the electrolyte.[99, 120]

On the other hand, the solubility of CO_2 in the electrolyte decreases at higher temperatures, and this leads to mass-transport limitations and favours the H_2O reduction reaction toward H_2. A decrease in the CO Faradic efficiency was observed at temperatures above 35° C (see Fig. 17a). However, by controlling both the current density and the CO_2 flow, it was possible to control the H_2/CO product ratio to between 1:4 and 9:1 (see Fig. 17b).[99]

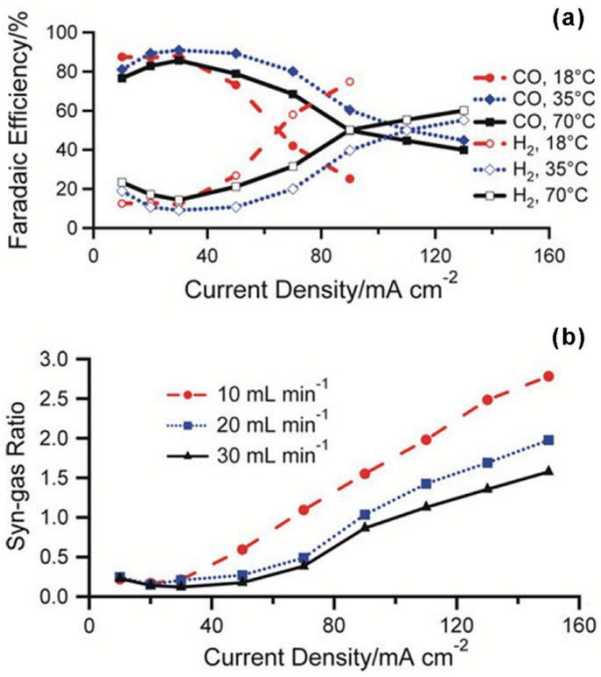

Figure 17. a) Cell performance at 18, 35 and 70 °C, CO_2 flow 20 mL min^{-1}: FE for CO and H_2; b) Syngas (H_2/CO) ratio as a function of the CO_2 flow rate, 0.8M K_2SO_4 catholyte, 70 °C. Adapted from Ref. [99] with the kind permission of Springer.

5.5. Pressure

Another aspect that has an important effect on the CO production rate is the CO_2 pressure. As described above, the higher the solubility of CO_2 is, the higher the feedstock concentration in the electrolyte and, as a result, the more CO will be produced. The main challenge concerning this kind of

View Article Online
DOI: 10.1039/C7GC00398F

experiment is the configuration of the reactor, which should be able to handle pressures of up to 30 bar.

A few research groups have studied CO_2 electro-reduction at high pressures. [47, 54, 121-123] Fig. 18 summarizes the CO current densities achieved with such high pressure systems. Hara *et al*.[47, 121] were among the first researchers to report the CO_2 reductions at 20 and 30 atm. They used a two-compartment electrochemical cell that was placed inside a stainless-steel autoclave. They achieved a current density as high as -300 $mA \cdot cm^{-2}$ by using Ag and Pd cathodes, and reached over 50 % of Faradaic efficiency for the CO production at 20 atm. Instead, working with Ag-based electrodes, they obtained a current density of -163 $mA \cdot cm^{-2}$ at -1.48 V *vs* Ag/AgCl with a Faradic efficiency to CO of 75.6 % at 30 bar. More recently, Dufek *et al*.[98] have recently reported a pressurized cell of the type shown in Fig. 10d (see Fig. 19) that operates with an Ag-based GDE. They achieved a CO_2 reduction to CO with a current density up to -225 $mA \cdot cm^{-2}$, by using pressurized CO_2 at 18.5 atm. With an 80 % Faradic efficiency, this system generated 5 times more CO at 20 bar than that at ambient pressure.

It is clear from Fig. 17 that although the increase in pressure plays a role in the production of CO, the catalytic material is the main player for a high conversion efficiency, and Ag and Pd are the most promising ones.

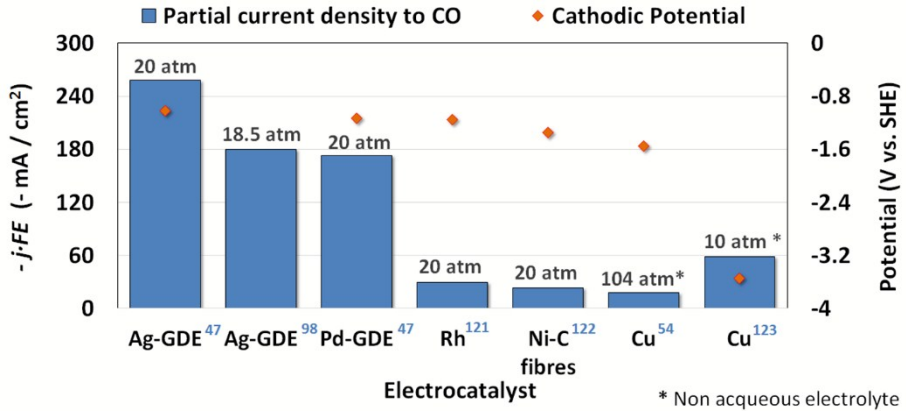

Figure 138. CO current densities and respective cathodic potentials for the reduction of CO_2 to CO in high pressure systems. The reference of each datum is given in the blue suffixes after the type of electrocatalyst.

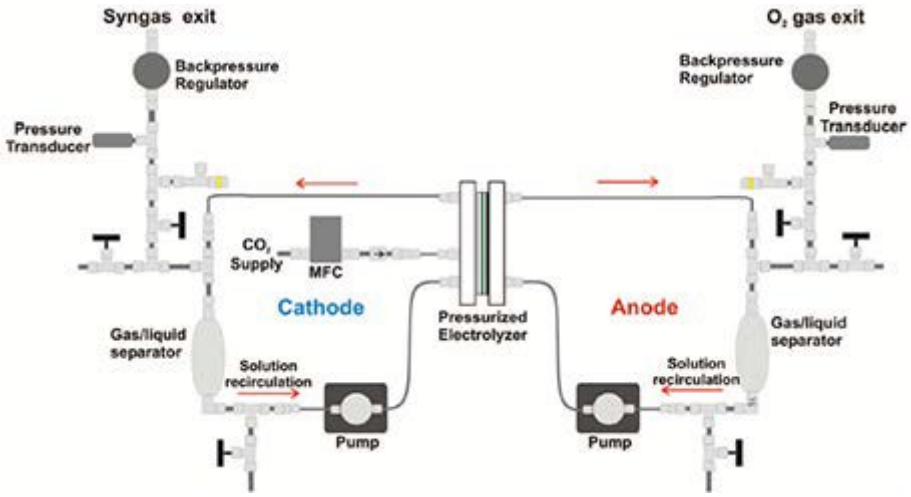

Figure 149. Schematic of the pressurized electrolysis system reported by Dufek *et al.* Reproduced from [98] with the kind permission of The Electrochemical Society. Copyright 2012.

5.6. Stability

The stability of a commercial electrochemical cell is a critical challenge. Although the Faradaic efficiency and current density are important factors to demonstrate the activity of a catalyst, a continuous production rate and the stability of the catalyst are other major factors for which there is still a lack of information in most reports and publications. Although high Faradaic efficiencies (more than 90 %) have already been reported in many works[33, 36, 50, 114, 118, 119, 124], these do not necessary result in a high production rate or a stable catalyst formulation. As can be seen in Fig. 20, there are neither results nor a discussion about the long-term results or stability of the catalyst in most of the reported experiments; moreover, even in the reports in which durability has been reported, the electrolysis had been conducted for less than 10 h.

The instability of CO_2 reduction catalysts has been observed, and this could be due to different phenomena. One reason could be superficial oxidation, in the case of metallic electrodes. The formation of a stable metal oxide coating on the surface of a catalyst can suppress the CO_2 adsorption and, as a result, a decay of the catalyst performance can be observed on these metal electrodes.[51] Therefore, the use of modified or deposited metals to avoid their passivation when they are either being prepared or under operation represents another interesting challenge. The active metal surface may oxidate, but this depends on the potential that is applied with respect to the electrochemical potential necessary for its oxidation. In this case, some of the active surface of the catalyst will be lost and, when a coating of metal nanoparticles is considered, problems can arise because of the metal loading on the surface of the electrode. Another possible reason for a degradation of the performance is the migration of H^+ to cathode when CEM is used, as previously reported, because when the cathode/electrolyte interface is particularly acidic, the CO_2 reduction reaction will be suppressed by the HER, with a consequent increase in the H_2/CO ratio.[38]

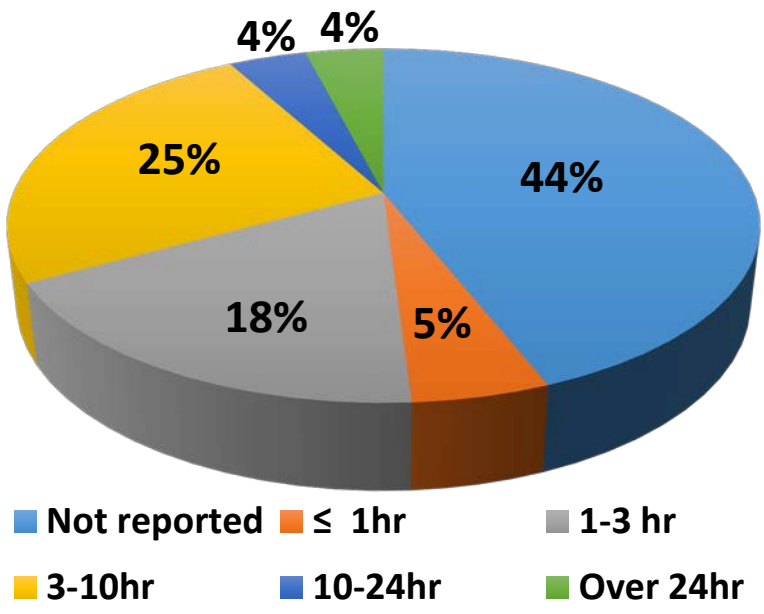

Figure 20. Duration of the experiments pertaining to the electrochemical reduction of CO_2 to CO.

View Article Online
DOI: 10.1039/C7GC00398F

6. Conclusions

The most recent efforts made to develop new technologies for the production of syngas through the electrochemical reduction of CO_2 to CO have been summarised. Catalysts play a key role in this process, and many reports have been written and methods have been used to enhance the yields and production rates of value-added products. The production of renewable syngas (CO, H_2) has gained a great deal of attention in recent years, due to its role in the production of other fuels, such as methane, methanol and other hydrocarbons, in order to substitute fossil-source derived alternatives. Although remarkable activities have been undertaken, and scientists have achieved high efficiency and selectivity with acceptable kinetics, there are still some serious obstacles to overcome before these processes can become viable. Although the current density values are not far from the values that are commonly used in industrial electrolysis applications, more efforts are needed to develop low-cost, efficient, selective and stable catalysis, in order to introduce this technology into an economic and viable process. The most efficient catalysts for the reduction of CO_2 to CO are based on the use of noble metals (*e.g*. Ag, Au, Pd). As a result, there is still a need for and the development of earth-abundant based heterogeneous catalysts with a low overpotential. In addition, new synthesis methods could be investigated to reduce the costs of catalysts. The stability of the catalysts is also a reason for concern: long-term tests and a complete understanding of the deactivation mechanisms have still not been reported or investigated for the most promising catalysts. These activities are essential to implement solutions that would allow the produced syngas to be used in downstream reactors in order to create value-added products (fuels or fine-chemicals). Finally, commercial processes generally convert thousands of moles per minute per cell,[33] whereas the proposed systems so far only produce CO in µmoles per minutes.

Different types of reactors have been used, and gas diffusion electrodes, which use different buffer layers or adjust the operation conditions (*i.e.* CO_2 flow rate, temperature, pressure), together with a tuning on the catalysts composition, would seem to represent a promising approach for the control of the H_2/CO ratio. Moreover, an accurate selection of the electrolytes can also enhance the CO_2 to CO reduction (*e.g.* larger cations favour the production of CO and suppress the evolution of H_2; high pHs could increase the overpotentials, but highly basic solution in GDE systems reduced ohmic drops and enhanced current). Hence, the efficient operation of the complete electrolytic system should be envisaged, from the anode to the PEM and to the cathode, and the whole system needs to be optimized through multiparametric approaches.

The reduction of CO_2 to value-added products, could pave the way towards a circular carbon-based economy, instead of Carbon Capture and Sequestration. Overall, there is already a good theoretical and experimental basis, but much work remains to be done before it will be possible for an efficient system to be applied.

Acknowledgments

This work has been funded by the EU Framework Program Horizon 2020 (H2020): Project CELBICON, Grant Agreement number 679050.

Supporting Information

Tables S1 to S3 containing the details of the conditions adopted in experiments made with different electrodes for the reduction of the CO_2 to CO and a short review of H_2 production electrocatalysts are reported in the supplementary Information. See DOI: 10.1039/x0xx00000x.

View Article Online
DOI: 10.1039/C7GC00398F

References

1. T. R. Karl and K. E. Trenberth, *Science*, 2003, 302, 1719-1723.
2. *IPCC, 2014: Climate Change 2014: Mitigation of Climate Change*, Cambridge University Press, United Kingdom and New York, NY, USA., 2014.
3. , ed. E. commission, United Nation, Paris, 2015.
4. G. A. Olah, A. Goeppert and G. K. S. Prakash, *J Org Chem*, 2009, 74, 487-498.
5. P. B. Kelemen and J. Matter, *Proceedings of the National Academy of Sciences*, 2008, 105, 17295-17300.
6. M. Aresta, A. Dibenedetto and A. Angelini, *Chem Rev*, 2014, 114, 1709-1742.
7. J. P. Jones, G. K. S. Prakash and G. A. Olah, *Isr J Chem*, 2014, 54, 1451-1466.
8. A. Q. Fenwick, J. M. Gregoire and O. R. Luca, *J. Photochem. Photobiol. B: Biol*, 2015, 152, 47-57.
9. C. Costentin, M. Robert and J. M. Saveant, *Chem Soc Rev*, 2013, 42, 2423-2436.
10. B. X. Hu, C. Guild and S. L. Suib, *J Co2 Util*, 2013, 2, 64-64.
11. R. J. Lim, M. S. Xie, M. A. Sk, J. M. Lee, A. Fisher, X. Wang and K. H. Lim, *Catal Today*, 2014, 233, 169-180.
12. B. Hu, C. Guild and S. L. Suib, *J Co2 Util*, 2013, 1, 18-27.
13. K. Li, X. An, K. H. Park, M. Khraisheh and J. Tang, *Catal Today*, 2014, 224, 3-12.
14. P. Akhter, M. A. Farkhondehfal, S. Hernández, M. Hussain, A. Fina, G. Saracco, A. U. Khan and N. Russo, *Journal of Environmental Chemical Engineering*, 2016, 4, 3934-3953.
15. C. Delacourt, P. L. Ridgway, J. B. Kerr and J. Newman, *J Electrochem Soc*, 2008, 155, B42-B49.
16. Syngas and Derivatives Market Trends: A Global Strategic Business Report, http://www.strategyr.com/MCP-7590.asp, Accessed Sept. 22nd, 2016.
17. R. M. I. Willner , D. Mandler , H. Durr , G. Dorr , K. Zengerle, *J Am Chem Soc*, 1987, 109.
18. K. Zhang, S. B. Wu, H. Yang, H. M. Yin and G. Li, *Rsc Adv*, 2016, 6, 77499-77506.
19. K. K. B.P. Sullivan , H.E. Guard, *Electrochemical and Electrocatalytic Reactions of Carbon Dioxide*, Elsevier B.V., 1993.
20. W. L. Zhu, R. Michalsky, O. Metin, H. F. Lv, S. J. Guo, C. J. Wright, X. L. Sun, A. A. Peterson and S. H. Sun, *J Am Chem Soc*, 2013, 135, 16833-16836.
21. A. J. F. Bard, Larry R, *Electrochemical Methods: Fundamentals and Applications*, wiley, 2001.
22. B. Kumar, M. Llorente, J. Froehlich, T. Dang, A. Sathrum and C. P. Kubiak, *Annu Rev Phys Chem*, 2012, 63, 541-569.
23. G. L. T. R.G. Lerner, *Encyclopaedia of Physics (2nd Edition*, VHC publishers, 1991.
24. A. S. D. T. Sawyer, and J. L. Roberts, *Electrochemistry for Chemists*, John Wiley, 1995.
25. J. Ronge, T. Bosserez, D. Martel, C. Nervi, L. Boarino, F. Taulelle, G. Decher, S. Bordiga and J. A. Martens, *Chem Soc Rev*, 2014, 43, 7963-7981.
26. F. Sastre, M. J. Munoz-Batista, A. Kubacka, M. Fernandez-Garcia, W. A. Smith, F. Kapteijn, M. Makkee and J. Gascon, *Chemelectrochem*, 2016, 3, 1497-1502.
27. C. Delacourt, P. L. Ridgway and J. Newman, *J Electrochem Soc*, 2010, 157, B1902-B1910.
28. E. Lamy, L. Nadjo and J. M. Saveant, *J Electroanal Chem*, 1977, 78, 403-407.
29. Y. Hori, A. Murata, K. Kikuchi and S. Suzuki, *J Chem Soc Chem Comm*, 1987, DOI: Doi 10.1039/C39870000728, 728-729.
30. Y. Hori, O. Koga, H. Yamazaki and T. Matsuo, *Electrochim Acta*, 1995, 40, 2617-2622.
31. Y. Hori, R. Takahashi, Y. Yoshinami and A. Murata, *J Phys Chem B*, 1997, 101, 7075-7081.
32. C. C. L. McCrory, S. Jung, I. M. Ferrer, S. M. Chatman, J. C. Peters and T. F. Jaramillo, *J Am Chem Soc*, 2015, 137, 4347-4357.
33. B. A. Rosen, A. Salehi-Khojin, M. R. Thorson, W. Zhu, D. T. Whipple, P. J. A. Kenis and R. I. Masel, *Science*, 2011, 334, 643-644.
34. J. H. Bang, K. Han, S. E. Skrabalak, H. Kim and K. S. Suslick, *J Phys Chem C*, 2007, 111, 10959-10964.
35. S. Sharma and B. G. Pollet, *J Power Sources*, 2012, 208, 96-119.

36. S. C. Ma, Y. C. Lan, G. M. J. Perez, S. Moniri and P. J. A. Kenis, *Chemsuschem*, 2014, 7, 866-874.
37. LIVE SPOT PRICES OF PRECIOUS METALS, https://www.bulliondesk.com/, Accessed January 06, 2016.
38. Y. Hori, H. Ito, K. Okano, K. Nagasu and S. Sato, *Electrochim Acta*, 2003, 48, 2651-2657.
39. F. Zhou, S. M. Liu, B. Q. Yang, P. X. Wang, A. S. Alshammari and Y. Q. Deng, *Electrochem Commun*, 2014, 46, 103-106.
40. F. K. F. Sastre A.V. Bavykina, M. Makkee and J. Gascon, *Submitted* 2016.
41. Q. Lu, J. Rosen, Y. Zhou, G. S. Hutchings, Y. C. Kimmel, J. G. G. Chen and F. Jiao, *Nat Commun*, 2014, 5.
42. H. T. Subiao Liu, Li Zeng, Qi Liu, Zhenghe Xu, Qingxia Liu, Jing-Li Luo, *J. Am. Chem. Soc*, 2017, 139, 4.
43. F. E. Osterloh, *Chem Soc Rev*, 2013, 42, 2294-2320.
44. J. W. Tang, J. R. Durrant and D. R. Klug, *J Am Chem Soc*, 2008, 130, 13885-13891.
45. S. C. Ma, R. Luo, J. I. Gold, A. Z. Yu, B. Kim and P. J. A. Kenis, *J Mater Chem A*, 2016, 4, 8573-8578.
46. C. E. Tornow, M. R. Thorson, S. Ma, A. A. Gewirth and P. J. A. Kenis, *J Am Chem Soc*, 2012, 134, 19520-19523.
47. K. Hara and T. Sakata, *B Chem Soc Jpn*, 1997, 70, 571-576.
48. M. Dunwell, J. H. Wang, Y. Yan and B. Xu, *Phys Chem Chem Phys*, 2017, 19, 971-975.
49. A. Wuttig, M. Yaguchi, K. Motobayashi, M. Osawa and Y. Surendranath, *P Natl Acad Sci USA*, 2016, 113, E4585-E4593.
50. Y. H. Chen, C. W. Li and M. W. Kanan, *J Am Chem Soc*, 2012, 134, 19969-19972.
51. K. Hara, A. Kudo, T. Sakata and M. Watanabe, *J Electrochem Soc*, 1995, 142, L57-L59.
52. C. W. Li, J. Ciston and M. W. Kanan, *Nature*, 2014, 508, 504-+.
53. C. W. Li and M. W. Kanan, *J Am Chem Soc*, 2012, 134, 7231-7234.
54. G. Y. Zhao, T. Jiang, B. X. Han, Z. H. Li, J. M. Zhang, Z. M. Liu, J. He and W. Z. Wu, *J Supercrit Fluid*, 2004, 32, 287-291.
55. R. Kas, K. K. Hummadi, R. Kortlever, P. de Wit, A. Milbrat, M. W. J. Luiten-Olieman, N. E. Benes, M. T. M. Koper and G. Mul, *Nat Commun*, 2016, 7.
56. J. F. Qing Li, Wenlei Zhu, Zhengzheng Chen, Bo Shen, Liheng Wu,Zheng Xi,Tanyuan Wang, Gang Lu, Jun-jie Zhu,Shouheng Sun, *J. Am. Chem. Soc*, 2017, DOI: 10.1021/jacs.7b00261.
57. J. Medina-Ramos, J. L. DiMeglio and J. Rosenthal, *J Am Chem Soc*, 2014, 136, 8361-8367.
58. S. A. Yao, R. E. Ruther, L. H. Zhang, R. A. Franking, R. J. Hamers and J. F. Berry, *J Am Chem Soc*, 2012, 134, 15632-15635.
59. D. Saravanakumar, J. Song, N. Jung, H. Jirimali and W. Shin, *Chemsuschem*, 2012, 5, 634-636.
60. J. D. Froehlich and C. P. Kubiak, *Inorg Chem*, 2012, 51, 3932-3934.
61. A. Parkin, J. Seravalli, K. A. Vincent, S. W. Ragsdale and F. A. Armstrong, *J Am Chem Soc*, 2007, 129, 10328-+.
62. S. W. Ragsdale, *Crit Rev Biochem Mol*, 2004, 39, 165-195.
63. N. Pentland, J. O. M. Bockris and E. Sheldon, *J Electrochem Soc*, 1957, 104, 182-194.
64. W. A. Badawy, H. E. Feky, N. H. Helal and H. H. Mohammed, *Int J Hydrogen Energ*, 2013, 38, 9625-9632.
65. P. D. Tran, T. V. Tran, M. Orio, S. Torelli, Q. D. Truong, K. Nayuki, Y. Sasaki, S. Y. Chiam, R. Yi, I. Honma, J. Barber and V. Artero, *Nat Mater*, 2016, 15, 640-646.
66. B. E. Conway and L. Bai, *J Chem Soc Farad T 1*, 1985, 81, 1841-&.
67. J. M. Jaksic, M. V. Vojnovic and N. V. Krstajic, *Electrochim Acta*, 2000, 45, 4151-4158.
68. A. Lasia and A. Rami, *J Electroanal Chem*, 1990, 294, 123-141.
69. M. Jaccaud, F. Leroux and J. C. Millet, *Mater Chem Phys*, 1989, 22, 105-119.
70. E. R. Kotz and S. Stucki, *J Appl Electrochem*, 1987, 17, 1190-1197.
71. S. Cobo, J. Heidkamp, P.-A. Jacques, J. Fize, V. Fourmond, L. Guetaz, B. Jousselme, V. Ivanova, H. Dau, S. Palacin, M. Fontecave and V. Artero, *Nat Mater*, 2012, 11, 802-807.

72. H. Cesiulis, N. Tsyntsaru, A. Budreika and N. Skridaila, *Surf Eng Appl Elect+*, 2010, 46, 406-415.
73. E. Gomez, E. Pellicer and E. Valles, *J Electroanal Chem*, 2001, 517, 109-116.
74. E. Gomez, E. Pellicer and E. Valles, *J Appl Electrochem*, 2003, 33, 245-252.
75. V. Kublanovsky, O. Bersirova, Y. Yapontseva, H. Cesiulis and E. Podlaha-Murphy, *Prot Met Phys Chem+*, 2009, 45, 588-594.
76. E. J. Podlaha and D. Landolt, *J Electrochem Soc*, 1996, 143, 885-892.
77. M. Spasojevic, N. Krstajic, P. Despotov, R. Atanasoski and K. Popov, *J Appl Electrochem*, 1984, 14, 265-266.
78. F. Safizadeh, E. Ghali and G. Houlachi, *Int J Hydrogen Energ*, 2015, 40, 256-274.
79. N. R. Elezovic, V. D. Jovic and N. V. Krstajic, *Electrochim Acta*, 2005, 50, 5594-5601.
80. R. K. Shervedani, A. H. Alinoori and A. R. Madram, *J New Mat Electr Sys*, 2008, 11, 259-265.
81. K. I. V. I. Arul Raj, *J Appl Electrochem*, 1990, 20, 32-38.
82. N. Danilovic, R. Subbaraman, D. Strmcnik, V. R. Stamenkovic and N. M. Markovic, *J Serb Chem Soc*, 2013, 78, 2007-2015.
83. M. Smiljanic, I. Srejic, B. Grgur, Z. Rakocevic and S. Strbac, *Electrocatalysis-Us*, 2012, 3, 369-375.
84. C. Cachet, M. Keddam, V. Mariotte and R. Wiart, *Electrochim Acta*, 1994, 39, 2743-2750.
85. A. Hamelin, *J Electroanal Chem*, 1996, 407, 1-11.
86. A. Hamelin and A. M. Martins, *J Electroanal Chem*, 1996, 407, 13-21.
87. A. Hamelin, L. Stoicoviciu, G. J. Edens, X. P. Gao and M. J. Weaver, *J Electroanal Chem*, 1994, 365, 47-57.
88. J. Perez, E. R. Gonzalez and H. M. Villullas, *J Phys Chem B*, 1998, 102, 10931-10935.
89. Y. H. Xu, *Int J Hydrogen Energ*, 2009, 34, 77-83.
90. L. A. Khanova and L. I. Krishtalik, *J Electroanal Chem*, 2011, 660, 224-229.
91. G. K. S. Prakash, F. A. Viva and G. A. Olah, *J Power Sources*, 2013, 223, 68-73.
92. E. A. Hernandez-Pagan, N. M. Vargas-Barbosa, T. Wang, Y. Zhao, E. S. Smotkin and T. E. Mallouk, *Energ Environ Sci*, 2012, 5, 7582-7589.
93. Y. C. Li, D. Zhou, Z. Yan, R. H. Gonçalves, D. A. Salvatore, C. P. Berlinguette and T. E. Mallouk, *ACS Energy Letters*, 2016, 1, 1149-1153.
94. K. P. Kuhl, E. R. Cave, D. N. Abram and T. F. Jaramillo, *Energ Environ Sci*, 2012, 5, 7050-7059.
95. T. Hatsukade, K. P. Kuhl, E. R. Cave, D. N. Abram and T. F. Jaramillo, *Phys Chem Chem Phys*, 2014, 16, 13814-13819.
96. K. N. Wu, E. Birgersson, B. Kim, P. J. A. Kenis and I. A. Karimi, *J Electrochem Soc*, 2015, 162, X6-X6.
97. K. Wu, E. Birgersson, B. Kim, P. J. A. Kenis and I. A. Karimi, *Journal of The Electrochemical Society*, 2015, 162, F23-F32.
98. E. J. Dufek, T. E. Lister, S. G. Stone and M. E. McIlwain, *J Electrochem Soc*, 2012, 159, F514-F517.
99. E. J. Dufek, T. E. Lister and M. E. McIlwain, *J Appl Electrochem*, 2011, 41, 623-631.
100. D. A. Vermaas, M. Sassenburg and W. A. Smith, *J Mater Chem A*, 2015, 3, 19556-19562.
101. H. Li and C. Oloman, *Journal of Applied Electrochemistry*, 2007, 37, 1107-1117.
102. R. L. Cook, R. C. Macduff and A. F. Sammells, *J Electrochem Soc*, 1990, 137, 187-189.
103. H. Mistry, R. Reske, Z. H. Zeng, Z. J. Zhao, J. Greeley, P. Strasser and B. R. Cuenya, *J Am Chem Soc*, 2014, 136, 16473-16476.
104. Z. Liu, R. I. Masel, Q. Chen, R. Kutz, H. Yang, K. Lewinski, M. Kaplun, S. Luopa and D. R. Lutz, *J Co2 Util*, 2016, 15, 50-56.
105. E. J. Dufek, T. E. Lister and M. E. McIlwain, *Electrochemical and Solid-State Letters*, 2012, 15, B48-B50.
106. Y. Hori, in *Modern Aspects of Electrochemistry*, eds. C. Vayenas, R. White and M. Gamboa-Aldeco, Springer New York, 2008, vol. 42, ch. 3, pp. 89-189.
107. H. R. Jhong, S. C. Ma and P. J. A. Kenis, *Curr Opin Chem Eng*, 2013, 2, 191-199.

108. Y. Hori, A. Murata and R. Takahashi, *Journal of the Chemical Society, Faraday Transactions 1: Physical Chemistry in Condensed Phases*, 1989, 85, 2309-2326.
109. M. Gattrell, N. Gupta and A. Co, *J Electroanal Chem*, 2006, 594, 1-19.
110. N. Gupta, M. Gattrell and B. MacDougall, *J Appl Electrochem*, 2006, 36, 161-172.
111. M. R. Thorson, K. I. Siil and P. J. A. Kenis, *J Electrochem Soc*, 2013, 160, F69-F74.
112. J. J. Wu, F. G. Risalvato, F. S. Ke, P. J. Pellechia and X. D. Zhou, *J Electrochem Soc*, 2012, 159, F353-F359.
113. D. Kopljar, N. Wagner and E. Klemm, *Chem Eng Technol*, 2016, 39, 2042-2050.
114. S. Verma, X. Lu, S. C. Ma, R. I. Masel and P. J. A. Kenis, *Phys Chem Chem Phys*, 2016, 18, 7075-7084.
115. B. Kim, S. Ma, H. R. M. Jhong and P. J. A. Kenis, *Electrochim Acta*, 2015, 166, 271-276.
116. A. Salehi-Khojin, H.-R. M. Jhong, B. A. Rosen, W. Zhu, S. Ma, P. J. A. Kenis and R. I. Masel, *The Journal of Physical Chemistry C*, 2013, 117, 1627-1632.
117. B. A. Rosen, A. Salehi-Khojin, M. R. Thorson, W. Zhu, D. T. Whipple, P. J. A. Kenis and R. I. Masel, *Science*, 2011, 334, 643-644.
118. M. Asadi, B. Kumar, A. Behranginia, B. A. Rosen, A. Baskin, N. Repnin, D. Pisasale, P. Phillips, W. Zhu, R. Haasch, R. F. Klie, P. Král, J. Abiade and A. Salehi-Khojin, *Nat Commun*, 2014, 5.
119. F. Zhou, S. Liu, B. Yang, P. Wang, A. S. Alshammari and Y. Deng, *Electrochemistry Communications*, 2014, 46, 103-106.
120. S. Hernández, G. Barbero, G. Saracco and A. L. Alexe-Ionescu, *The Journal of Physical Chemistry C*, 2015, 119, 9916-9925.
121. K. Hara, A. Kudo and T. Sakata, *Journal of Electroanalytical Chemistry*, 1995, 391, 141-147.
122. T. Yamamoto, D. A. Tryk, K. Hashimoto, A. Fujishima and M. Okawa, *J Electrochem Soc*, 2000, 147, 3393-3400.
123. S. Kaneco, K. Iiba, H. Katsumata, T. Suzuki and K. Ohta, *Chem Eng J*, 2007, 128, 47-50.
124. C. Costentin, S. Drouet, M. Robert and J. M. Saveant, *Science*, 2012, 338, 90-94.

View Article Online
DOI: 10.1039/C7GC00398F

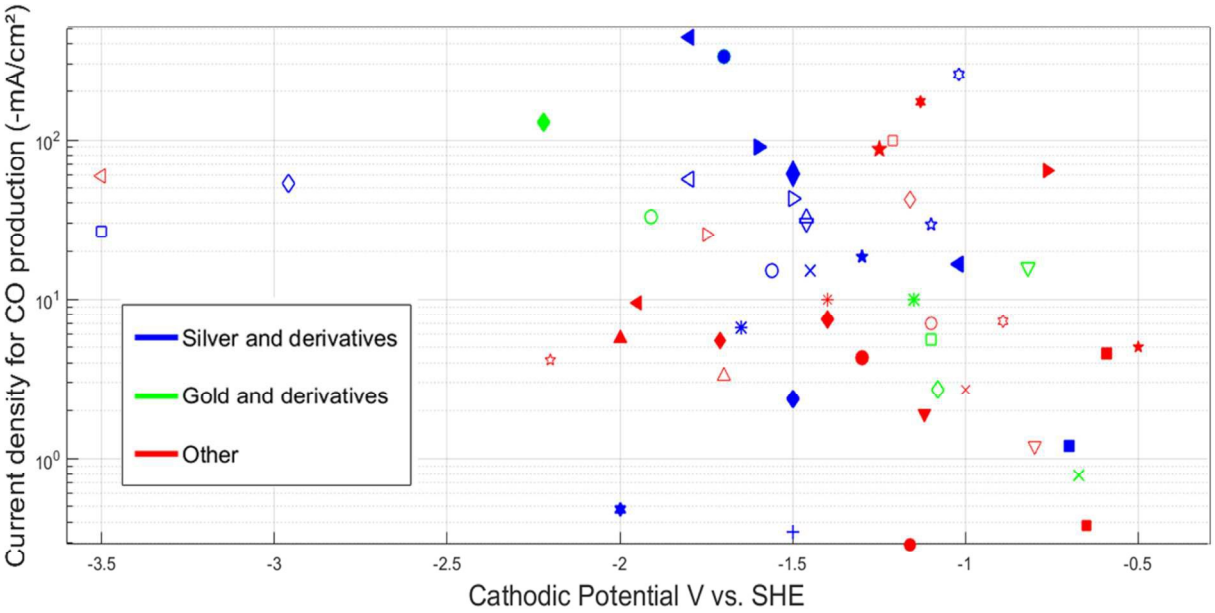

The opportunities and challenges for exploiting the production of Syngas from the electrochemical reduction of CO_2 are critically reviewed and analysed.